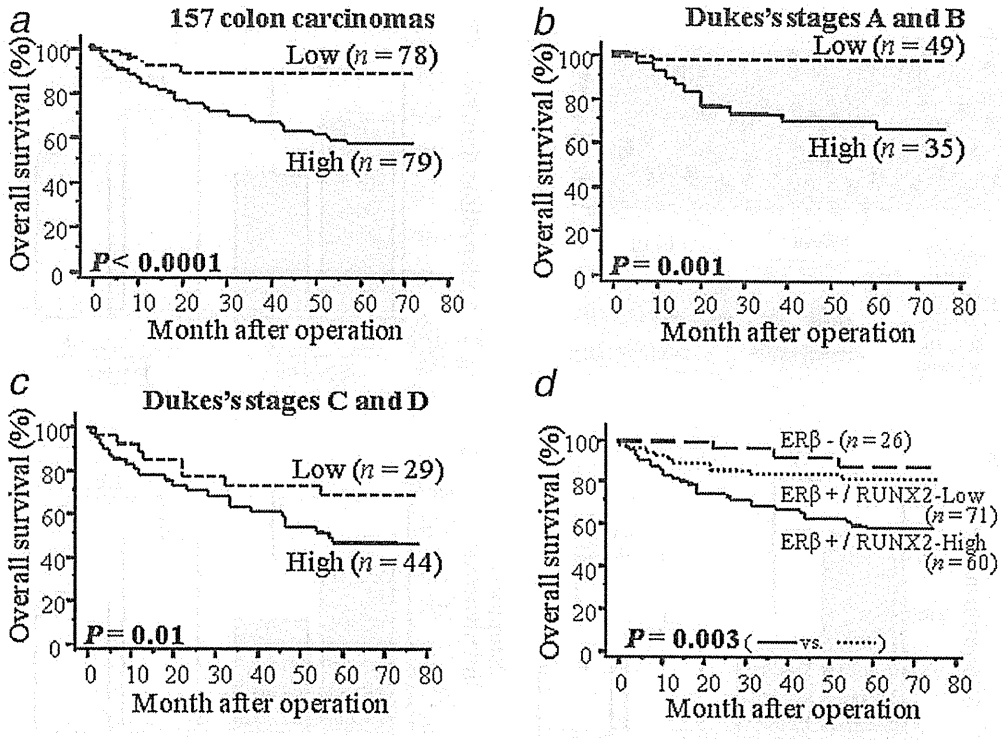

Figure 2. Overall survival curves of 157 colon carcinoma patients according to the RUNX2 immunoreactivity by Kaplan–Meier method. (*a*) RUNX2 immunoreactivity was significantly associated with worse prognosis (p <0.0001 by the log-rank test), when RUNX2 LI was further classified into two groups according to the median value. (*b* and *c*) Similar tendency was also detected in the patient groups of Dukes' stages *a* and *b* (*b*: $n = 84$) and the groups of Dukes' stages *c* and *d* (C: $n = 73$). (*d*) An association between ERβ status and clinical outcome of the patients according to the status of RUNX2 immunoreactivity. ERβ-positive cases were further categorized into two subgroups according to the median value of RUNX2 LI. Significant association ($p = 0.003$) was detected between ERβ+/RUNX2-High and ERβ+/RUNX2-Low groups.

Table 2. Univariate and multivariate analysis of overall survival of 157 colon carcinoma patients

	Univariate		Multivariate
Variable	*p*	*p*	Hazard ratio (95% CI)
RUNX2 LI (high/low)[1]	<0.0001[2]	0.003	1.0 (1.0–1.1)
Liver metastasis (+/−)	<0.0001[2]	0.05	
Ki67 LI (high/low)[1]	0.01[2]	0.02	1.0 (0.9–1.0)
Lymph node metastasis (+/−)	0.03[2]	0.62	
ERβ (+/−)	0.04[2]	0.20	
Gender (women/men)	0.13		
Histological differentiation[3] (moderate + poor/well)	0.51		

[1]The cases were categorized into two groups according to the median value.[26] [2]Data were considered significant in univariate analysis, and were examined in multivariate analysis. [3]Cases of mucinous adenocarcinoma were excluded in this study ($n = 147$). Statistically significant values ($p < 0.05$) were in boldface.

in the cell block in these cell lines was 67.4 and 81.8%, respectively (Fig. 3*a*, upper panel). RUNX2 mRNA expression level was markedly decreased in these cells transfected with specific siRNA against RUNX2 both at 2 and 4 days after the transfection compared to those transfected with control siRNA, and the ratio of RUNX2 mRNA level compared to that in the control siRNA at 2 and 4 days was 14.1 and 3.6% in SW480 and 7.8 and 5.9% in DLD-1 cells, respectively. Immunoblotting analysis subsequently confirmed decreased RUNX2 protein expression in SW480 and DLD1 cells transfected with RUNX2 siRNA for 3 days (Fig. 3*a*, lower panel).

As demonstrated in Figure 3*b*, cell proliferative activity was significantly lower both in SW480 and DLD-1 cells transfected with siRNA against RUNX2 ($p < 0.01$ and 0.74-fold in SW480, and $p < 0.01$ and 0.83-fold in DLD-1) than those transfected with control siRNA at 3 days after the transfection. In the migration assay, the migration area was significantly decreased in these cells transfected with siRNA against RUNX2 at 1 day after scratch (SW480: $p < 0.001$ and 0.43-fold, and DLD-1: $p < 0.001$ and 0.63-fold; Figure 3*c* and Supporting Information Fig. S1). In addition, the number of invading cells was significantly lower in the cells transfected with RUNX2 siRNA than those transfected with control siRNA at 3 days after the transfection (SW480: $p < 0.05$ and 0.69-fold, and DLD-1: $p < 0.01$ and 0.66-fold; Fig. 3*d*).

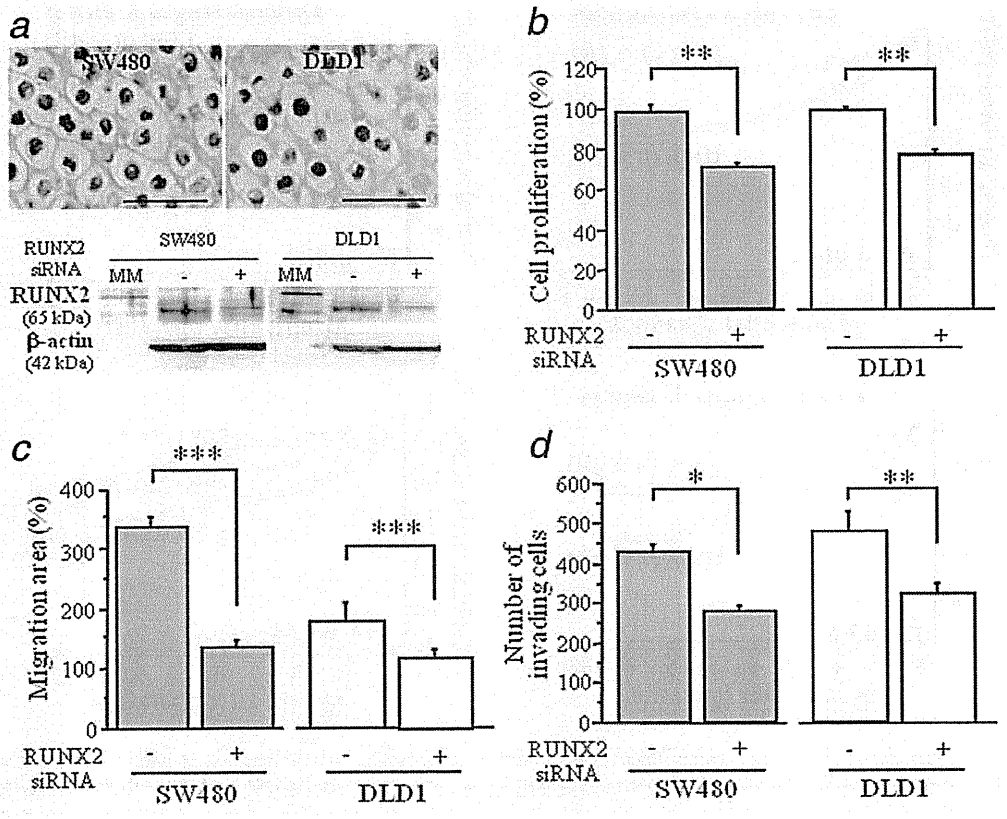

Figure 3. Effects of RUNX2 expression on cell proliferation, migration and invasive properties in colon carcinoma cells. (*a*) Expression of RUNX2 protein in SW480 and DLD1 cells. Upper panel demonstrated results of immunocytochemistry of RUNX2 in SW480 (left upper panel) and DLD-1 (right upper panel) cells. Cell blocks from formalin-fixed and paraffin-embedded specimens, and bar = 50 μm, respectively. Lower panel demonstrated immunoblotting of RUNX2 in SW480 (left lower panel) and DLD1 (right lower panel) cells transfected with specific RUNX2 siRNA (*i.e.*, RUNX2 siRNA: +) or control siRNA (*i.e.*, RUNX2 siRNA: –). The protein of cells was extracted at 3 days after the transfection. MM: molecular marker. (*b–d*): Results of proliferation (*b*), migration (*c*) and invasion (*d*) assays in SW480 (gray bar) and DLD-1 (open bar) cells were summarized. These cells were transfected with specific RUNX2 siRNA or control siRNA. Data were presented as mean ± SD ($n = 3$), respectively. *; $p < 0.05$, **; $p < 0.01$ and ***; $p < 0.001$. The statistical analyses were performed using Student's *t* test. [Color figure can be viewed in the online issue, which is available at wileyonlinelibrary.com.]

Regulation of RUNX2 expression by ERβ in colon carcinoma cells

As described earlier, RUNX2 immunoreactivity was positively associated with ERβ status in colon carcinomas examined (Table 1 and Fig. 1*f*), which suggests a possible interaction of RUNX2 and ERβ in colon carcinoma cells. Therefore, to further investigate this interaction, we treated the cells positive for ERβ but negative for ERα with a pure ER antagonist ICI 182,780.[27,28] As summarized in Figures 4*a* and 4*b*, ICI 182,780 significantly inhibited the RUNX2 mRNA level of these cells in a dose-dependent manner, significant at 5 μM of ICI 182,780 treatment compared to the basal level (SW480: $p < 0.05$ and 0.26-fold, DLD-1: $p < 0.05$ and 0.21-fold). RUNX2 mRNA level was also significantly ($p < 0.05$, respectively) suppressed in SW480 (0.66-fold) and DLD1 (0.68-fold) cells transfected with ERβ siRNA (Fig. 4*c*). Conversely, ERβ mRNA level itself was not significantly different (SW480: $p = 0.18$ and 0.89-fold, and DLD-1: $p = 0.96$ and 0.98-fold) between the cells treated with RUNX2 and control siRNA (Fig. 4*d*).

When SW480 and DLD1 cells were treated with 5 μM of ICI 182,780 for 3 days, their cell proliferation and invasive properties were both significantly suppressed compared to the control or nontreated cells [cell proliferation activity: $p < 0.01$ in SW480 and $p < 0.05$ in DLD1 (Supporting Information Fig. S2A), and invasive property: $p = 0.12$ in SW480 and $p < 0.05$ in DLD1 (Supporting Information Fig. S2B)].

Discussion

In this study, we first demonstrated that RUNX2 immunoreactivity was frequently detected in colon carcinoma cells but negligible in non-neoplastic colonic mucosa and turned out

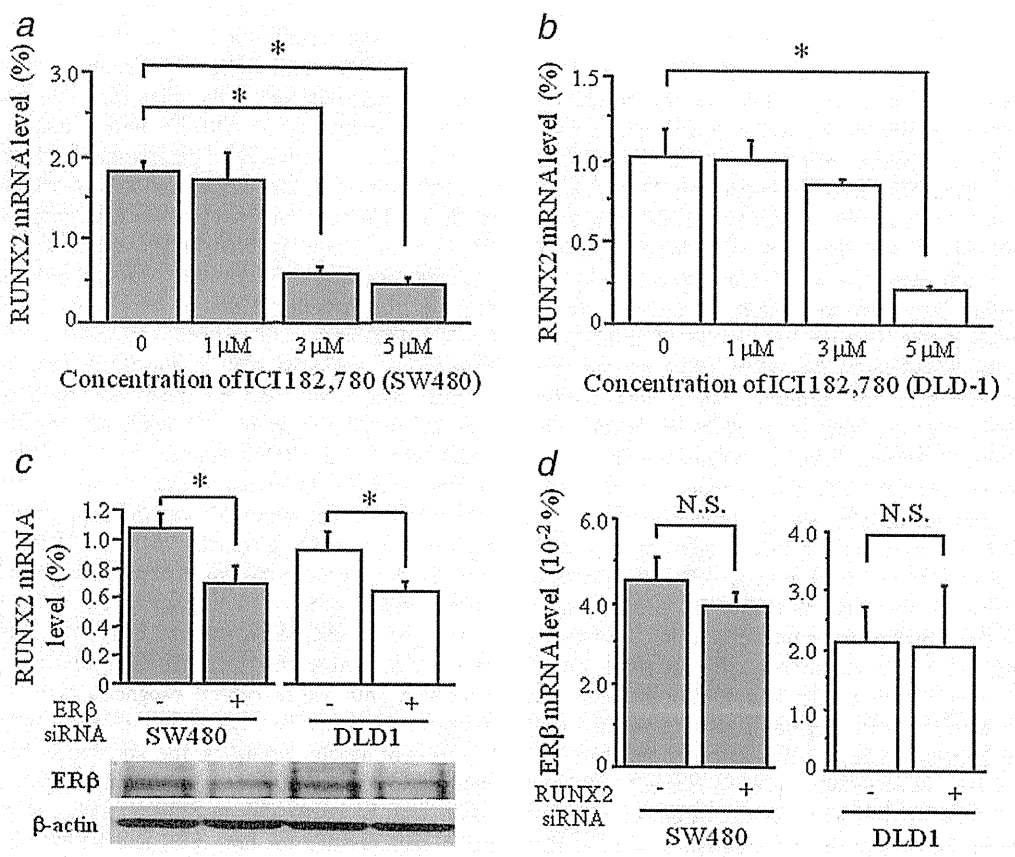

Figure 4. Regulation of RUNX2 expression in colon carcinoma cells. (*a* and *d*) Effects of ICI 182,780 on RUNX2 mRNA expression in SW480 (*a*) and DLD-1 (*b*) cells by real-time PCR analysis. The cells were treated with indicated concentrations of ICI 182,780 for 3 days. (*c*) Effects of ERβ siRNA on RUNX2 mRNA expression in SW480 (gray bar) and DLD-1 (open bar) cells. These cells were transfected with specific ERβ siRNA (ERβ siRNA: +) or control siRNA (ERβ siRNA: −), and RUNX2 mRNA level was examined using real-time PCR analysis. Data were presented as mean ± SD ($n = 3$), respectively. *; $p < 0.05$, and the statistical analyses were performed using Student's *t* test. Lower panel summarized ERβ protein level in each specimens according to the results of immunoblot analysis. (*d*) Effects of RUNX2 on ERβ mRNA expression in SW480 (gray bar) and DLD-1 (open bar) cells. ERβ mRNA level was evaluated by real-time PCR analysis in the cells treated with specific RUNX2 siRNA (RUNX2 siRNA: +) or control siRNA (RUNX2 siRNA: −). Data were presented mean ± SD ($n = 3$), respectively. *; $p < 0.05$, and N.S.; not significant. The statistical analyses were performed using one-way ANOVA and Bonferroni test (*a* and *b*) or Student's *t* test (*c* and *d*).

as an independent adverse prognostic factor of the patients. RUNX2 immunolocalization was previously reported in prostate,[11] pancreatic,[12] thyroid[13] and breast[14] carcinoma tissues. RUNX2 expression was also reported to be elevated in carcinoma cells compared to normal epithelium in both pancreatic and breast carcinoma, and was significantly associated with adverse clinical outcome in breast carcinoma patients.[12,14] Results of our present study in colon carcinoma are in general consistent with results of these reports above and suggest that RUNX2 immunoreactivity in carcinoma cells serves as a potent marker of aggressive clinical behavior in colon carcinoma patients.

In our present study, RUNX2 immunoreactivity was positively associated with Dukes' stage and liver metastasis in colon carcinoma patients. Results of the subsequent *in vitro* experiments also indicated that RUNX2 significantly promoted cell proliferation, migration and invasive properties of colon carcinoma cells. The processes of carcinoma metastasis generally consist of multisteps including migration, invasion, dissemination into the blood vessel and proliferation at the site of metastatic organ and the metastasis is the greatest cause of death in colon carcinoma patients. Results of previously reported *in vitro* studies demonstrated that RUNX2 expression induced the cell proliferation of mouse[15] and rat[16] colon carcinoma cell lines. RUNX2 stimulated transcription of osteopontin, which was also reported to increase metastatic properties in human colon carcinoma cells[29] and CT26 mouse colorectal carcinoma cells.[15] However, it is also true

that RUNX2 expression was recently reported to be modulated by TGF-β1 in CC531 rat colorectal carcinoma cells,[16] which subsequently induced angiogenesis and metastasis of colon carcinoma.[30] RUNX2 expression was also reported to be closely associated with the expression of vascular endothelial growth factor,[31] matrix metalloproteinase[32,33] and bone sialoprotein.[34] Therefore, it is suggested that RUNX2 plays important roles in the growth and metastasis of colon carcinoma cells through its wide spectrums of biological functions. However, it is also true that RUNX2 immunoreactivity was not significantly associated with depth of invasion, lymph node metastasis, peritoneal metastasis or Ki67 LI in the colon carcinoma cases examined in this study, which was not necessarily consistent with the results of our *in vitro* studies. Further examinations are required to clarify the precise molecular functions of RUNX2 in colon carcinoma cells.

Results of our present study demonstrated that the status of RUNX2 immunoreactivity was positively associated with that of ERβ in colon carcinoma cells, suggesting a possible interaction of RUNX2 and ERβ in these cells. ER consists of ERα and ERβ in humans, and ERβ is predominantly expressed in some malignancies including colon,[35] while the great majority of breast carcinoma cells expresses ERα.[36] Das *et al.*[37] reported that ERα and ERβ expression was decreased in MCF-7 breast carcinoma cells transfected with RUNX2, but Matsumoto *et al.*[38] demonstrated that estradiol enhanced bone morphologic protein-induced RUNX2 expression in ERα and ERβ positive C2C12 mouse myoblast cells. Results of our present *in vitro* studies also showed that RUNX2 mRNA expression was decreased by ICI 182,780 both in SW480 and DLD-1 colon carcinoma cells in a dose-dependent manner but the level of ERβ mRNA expression was not significantly changed in these cells transfected with RUNX2 siRNA. SW480 and DLD-1 cells used in our present study have been known negative for ERα but positive for ERβ,[27,28] and ICI 182,780 is a well-characterized pure antagonist of ERs.[39,40] Very recently, Edvardsson *et al.*[17] reported that ERβ induced RUNX2 expression through its direct binding to the promoter in colorectal carcinoma cells, which is consistent with results of our present study. Therefore, these findings above all suggest that RUNX2 expression is at least reasonably postulated to be partly upregulated by estrogenic signals through ERβ in colon carcinoma cells.

Results of previous studies regarding estrogen actions in colon carcinoma cells are in general inconsistent in terms of its biological actions and its significance has still remained unclear. Results of various epidemiological studies have generally suggested a protective effect of hormone replacement therapy on the risk of developing colorectal carcinomas, which also implied that estrogen exerts a protective effect against colorectal cancer in relatively early stage of carcinoma development.[41] However, Janakiram *et al.*[42] reported that ERβ acted as a colon tumor promoter and raloxifene, a selective ER modulator, protected colon carcinogenesis. In addition, we previously demonstrated that intratumoral estrogen levels were significantly higher than those in non-neoplastic colonic mucosa, and were significantly associated with adverse clinical outcome of the colon carcinoma patients.[43]

Clinical significance of ERβ has been proposed in the colon carcinomas, but has not been necessarily determined. An association between loss of ERβ and adverse clinicopathological factors has been reported by several investigators,[44–46] but Wong *et al.*[35] reported that higher expression of ERβ was positively associated with the presence of lymph node metastasis in the patients. Little is known on an association between ERβ status and prognosis of colon carcinoma, and Fang *et al.*[47] reported ERβ as the better prognostic factor, whereas, Sato *et al.*[43] did not detect any significant correlation. In our present study, ERβ status was significantly associated with worse clinical outcome of 157 colon carcinoma patients, and results of our present *in vitro* studies demonstrated that ER antagonist ICI 182,780 suppressed cell proliferation and invasive properties of both SW480 and DLD1 cells. ER is in general known to activate the transcription of various target genes and estrogenic functions are usually determined by expression patterns or profiles of these target genes. Considering the fact that high RNUN2 group was associated with worse clinical prognosis than low RUNX2 group in ERβ-positive cases in our present study (Fig. 2*d*), inconsistent results regarding the correlation between ERβ status and clinical outcome of colon carcinoma patients above may be partly due to different ratios of colon carcinoma cells positive for both ERβ and RUNX2 examined in their cohorts.

In summary, RUNX2 immunoreactivity was frequently detected in colon carcinoma tissues, and the median value of RUNX2 LI was 67% in our present study. The RUNX2 LI was positively associated with Dukes' stage, liver metastasis and ERβ status of the patients and turned out as an independent prognostic factor of these patients. Results of our *in vitro* studies also demonstrated that both SW480 and DLD-1 human colon carcinoma cells transfected with specific siRNA against RUNX2 significantly decreased the cell proliferation, migration and invasive properties of carcinoma cells. In addition, RUNX2 mRNA expression was significantly inhibited by a pure ER antagonist ICI 182,780 in these cells positive for ERβ. These *in vivo* and *in vitro* findings suggest that RUNX2 is a potent prognostic factor in human colon carcinoma patients through the promotion of cell proliferation, migration and invasive properties of carcinoma cells and its expression may at least be partly induced by estrogen signals through ERβ.

Acknowledgements

The authors appreciate the skillful technical assistance of Mr. Katsuhiko Ono (Department of Pathology, Tohoku University Graduate School of Medicine, Sendai, Japan), Dr. Akihiro Yamamura, Dr. Kyouhei Ariake, Ms. Emiko Shibuya, Ms. Keiko Inabe, and Ms. Hiroko Fujimura (Department of Surgery, Tohoku University Graduate School of Medicine, Sendai, Japan, respectively).

References

1. American Cancer Society. Cancer facts & figures 2007. Atlanta: American Cancer Society, 2007.
2. Colucci G, Gebbia V, Paoletti G, Giuliani F, Caruso M, Gebbia N, Cartenì G, Agostara B, Pezzella G, Manzione L, Borsellino N, Misino A, et al. Phase III randomized trial of FOLFIRI versus FOLFOX4 in the treatment of advanced colorectal cancer: a multicenter study of the Gruppo Oncologico Dell'Italia Meridionale. *J Clin Oncol* 2005;23:4866–75.
3. Ito Y. Oncogenic potential of the RUNX gene family: 'Overview'. *Oncogene* 2004;23: 4198–208.
4. Ducy P, Zhang R, Geoffroy V, Ridall AL, Karsenty G. Osf2/Cbfa1: a transcriptional activator of osteoblast differentiation. *Cell* 1997;89:747–54.
5. Komori T, Yagi H, Nomura S, Yamaguchi A, Sasaki K, Deguchi K, Shimizu Y, Bronson RT, Gao YH, Inada M, Sato M, Okamoto R et al. Targeted disruption of Cbfa1 results in a complete lack of bone formation owing to maturational arrest of osteoblasts. *Cell* 1997;89:755–64.
6. Otto F, Thornell AP, Crompton T, Denzel A, Gilmour KC, Rosewell IR, Stamp GW, Beddington RS, Mundlos S, Olsen BR, Selby PB, Owen MJ. Cbfa1, a candidate gene for cleidocranial dysplasia syndrome, is essential for osteoblast differentiation and bone development. *Cell* 1997;89: 765–71.
7. Mundlos S, Otto F, Mundlos C, Mulliken JB, Aylsworth AS, Albright S, Lindhout D, Cole WG, Henn W, Knoll JH, Owen MJ, Mertelsmann R, et al. Mutations involving the transcription factor CBFA1 cause cleidocranial dysplasia. *Cell* 1997;89:773–9.
8. Zheng Q, Zhou G, Morello R, Chen Y, Garcia-Rojas X, Lee B. Type X collagen gene regulation by Runx2 contributes directly to its hypertrophic chondrocyte-specific expression in vivo. *J Cell Biol* 2003; 162:833–42.
9. San Martin IA, Varela N, Gaete M, Villegas K, Osorio M, Tapia JC, Antonelli M, Mancilla EE, Pereira BP, Nathan SS, Lian JB, Stein JL, et al. Impaired cell cycle regulation of the osteoblast-related heterodimeric transcription factor Runx2-Cbfbeta in osteosarcoma cells. *J Cell Physiol* 2009;221:560–71.
10. Pereira BP, Zhou Y, Gupta A, Leong DT, Aung KZ, Ling L, Pho RW, Galindo M, Salto-Tellez M, Stein GS, Cool SM, van Wijnen AJ, et al. Runx2, p53, and pRB status as diagnostic parameters for deregulation of osteoblast growth and differentiation in a new pre-chemotherapeutic osteosarcoma cell line (OS1). *J Cell Physiol* 2009;221:778–88.
11. Brubaker KD, Vessella RL, Brown LG, Corey E. Prostate cancer expression of runt-domain transcription factor Runx2, a key regulator of osteoblast differentiation and function. *Prostate* 2003;56:13–22.
12. Kayed H, Jiang X, Keleg S, Jesnowski R, Giese T, Berger MR, Esposito I, Löhr M, Friess H, Kleeff J. Regulation and functional role of the Runt-related transcription factor-2 in pancreatic cancer. *Br J Cancer* 2007;97:1106–15.
13. Endo T, Ohta K, Kobayashi T. Expression and function of Cbfa-1/Runx2 in thyroid papillary carcinoma cells. *J Clin Endocrinol Metab* 2008;93:2409–12.
14. Onodera Y, Miki Y, Suzuki T, Takagi K, Akahira J, Sakyu T, Watanabe M, Inoue S, Ishida T, Ohuchi N, Sasano H. Runx2 in human breast carcinoma: its potential roles in cancer progression. *Cancer Sci* 2010;101: 2670–5.
15. Wai PY, Mi Z, Gao C, Guo H, Marroquin C, Kuo PC. Ets-1 and runx2 regulate transcription of a metastatic gene, osteopontin, in murine colorectal cancer cells. *J Biol Chem* 2006;281:18973–82.
16. Georges R, Adwan H, Zhivkova M, Eyol E, Bergmann F, Berger MR. Regulation of osteopontin and related proteins in rat CC531 colorectal cancer cells. *Int J Oncol* 2010;37:249–56.
17. Edvardsson K, Ström A, Jonsson P, Gustafsson JÅ, Williams C. Estrogen receptor β induces antiinflammatory and antitumorigenic networks in colon cancer cells. *Mol Endocrinol* 2011;25:969–79.
18. Mak IW, Cowan RW, Popovic S, Colterjohn N, Singh G, Ghert M. Upregulation of MMP-13 via Runx2 in the stromal cell of Giant Cell Tumor of bone. *Bone* 2009;45:377–86.
19. Allred DC, Clark GM, Elledge R, Fuqua SA, Brown RW, Chamness GC, Osborne CK, McGuire WL. Association of p53 protein expression with tumor cell proliferation rate and clinical outcome in node-negative breast cancer. *J Natl Cancer Inst* 1993;85:200–6.
20. Howell A, Osborne CK, Morris C, Wakeling AE. ICI 182,780 (Faslodex): development of a novel, "pure" antiestrogen. *Cancer* 2000;89:817–25.
21. Dumoulin FL, Nischalke HD, Leifeld L, von dem Bussche A, Rockstroh JK, Sauerbruch T, Spengler U. Semi-quantification of human C-C chemokine mRNAs with reverse transcription/real-time PCR using multi-specific standards. *J Immunol Methods* 2000;241:9–19.
22. Miki Y, Suzuki T, Hatori M, Igarashi K, Aisaki KI, Kanno J, Nakamura Y, Uzuki M, Sawai T, Sasano H. Effects of aromatase inhibitors on human osteoblast and osteoblast-like cells: a possible androgenic bone protective effects induced by exemestane. *Bone* 2007;40:876–87.
23. Suzuki T, Inoue A, Miki Y, Moriya T, Akahira J, Ishida T, Hirakawa H, Yamaguchi Y, Hayashi S, Sasano H. Early growth responsive gene 3 in human breast carcinoma: a regulator of estrogen-meditated invasion and a potent prognostic factor. *Endocr Relat Cancer* 2007;14: 279–92.
24. Fang YJ, Pan ZZ, Li LR, Lu ZH, Zhang LY, Wan DS. MMP7 expression regulated by endocrine therapy in ERbeta-positive colon cancer cells. *J Exp Clin Cancer Res* 2009;28: 132–9.
25. Ehrhardt GR, Hijikata A, Kitamura H, Ohara O, Wang JY, Cooper MD. Discriminating gene expression profiles of memory B cell subpopulations. *J Exp Med* 2008;205:1807–17.
26. Fluge Ø, Gravdal K, Carlsen E, Vonen B, Kjellevold K, Refsum S, Lilleng R, Eide TJ, Halvorsen TB, Tveit KM, Otte AP, Akslen LA, et al. Expression of EZH2 and Ki-67 in colorectal cancer and associations with treatment response and prognosis. *Br J Cancer* 2009;101:1282–9.
27. Arai N, Strom A, Rafter JJ, Gustafsson JA. Estrogen receptor beta mRNA in colon cancer cells: growth effects of estrogen and genistein. *Biochem Biophys Res Commun* 2000;270:425–31.
28. Lauber SN, Ali S, Gooderham NJ. The cooked food derived carcinogen 2-amino-1-methyl-6-phenylimidazo[4,5-b] pyridine is a potent oestrogen: a mechanistic basis for its tissue-specific carcinogenicity. *Carcinogenesis* 2004;12:2509–17.
29. Likui W, Hong W, Shuwen Z. Clinical significance of the upregulated osteopontin mRNA expression in human colorectal cancer. *J Gastrointest Surg* 2010; 14:74–81.
30. Bellone G, Carbone A, Tibaudi D, Mauri F, Ferrero I, Smirne C, Suman F, Rivetti C, Migliaretti G, Camandona M, Palestro G, Emanuelli G, et al. Differential expression of transforming growth factors-beta1, -beta2 and -beta3 in human colon carcinoma. *Eur J Cancer* 2001;37:224–33.
31. Zelzer E, Glotzer DJ, Hartmann C, Thomas D, Fukai N, Soker S, Olsen BR. Tissue specific regulation of VEGF expression during bone development requires Cbfa1/Runx2. *Mech Dev* 2001;106:97–106.
32. Pratap J, Javed A, Languino LR, van Wijnen AJ, Stein JL, Stein GS, Lian JB. The Runx2 osteogenic transcription factor regulates matrix metalloproteinase 9 in bone metastatic cancer cells and controls cell invasion. *Mol Cell Biol* 2005;25: 8581–91.

33. Selvamurugan N, Kwok S, Partridge NC. Smad3 interacts with JunB and Cbfa1/Runx2 for transforming growth factor-beta1-stimulated collagenase-3 expression in human breast cancer cells. *J Biol Chem* 2004;279:27764–73.
34. Barnes GL, Javed A, Waller SM, Kamal MH, Hebert KE, Hassan MQ, Bellahcene A, Van Wijnen AJ, Young MF, Lian JB, Stein GS, Gerstenfeld LC. Gerstenfeld LC. Osteoblast-related transcription factors Runx2 (Cbfa1/AML3) and MSX2 mediate the expression of bone sialoprotein in human metastatic breast cancer cells. *Cancer Res* 2003;63:2631–7.
35. Wong NA, Malcomson RD, Jodrell DI, Groome NP, Harrison DJ, Saunders PT. ERβ isoform expression in colorectal carcinoma: an in vivo and in vitro study of clinicopathological and molecular correlates. *J Pathol* 2005;207:53–60.
36. Ali S, Coombes RC. Estrogen receptor alpha in human breast cancer: occurrence and significance. *J Mammary Gland Biol Neoplasia* 2000;5:271–81.
37. Das K, Leong DT, Gupta A, Shen L, Putti T, Stein GS, van Wijnen AJ, Salto-Tellez M. Positive association between nuclear Runx2 and oestrogen-progesterone receptor gene expression characterises a biological subtype of breast cancer. *Eur J Cancer* 2009;45; 2239–48.
38. Matsumoto Y, Otsuka F, Takano M, Mukai T, Yamanaka R, Takeda M, Miyoshi T, Inagaki K, Sada KE, Makino H. Estrogen and glucocorticoid regulate osteoblast differentiation through the interaction of bone morphogenetic protein-2 and tumor necrosis factor-alpha in C2C12 cells. *Mol Cell Endocrinol* 2010;325; 118–127.
39. Howell A, Robertson JF, Quaresma Albano J, Aschermannova A, Mauriac L, Kleeberg UR, Vergote I, Erikstein B, Webster A, Morris C. Fulvestrant, formerly ICI 182,780, is as effective as anastrozole in postmenopausal women with advanced breast cancer progressing after prior endocrine treatment. *J Clin Oncol* 2002;20: 3396–403.
40. Niikawa H, Suzuki T, Miki Y, Suzuki S, Nagasaki S, Akahira J, Honma S, Evans DB, Hayashi S, Kondo T, Sasano H. Intratumoral estrogens and estrogen receptors in human non-small cell lung carcinoma. *Clin Cancer Res* 2008;14: 4417–26.
41. Chen MJ, Longnecker MP, Morgenstern H, Lee ER, Frankl HD, Haile RW. Recent use of hormone replacement therapy and the prevalence of colorectal adenomas. *Cancer Epidemiol Biomarkers Prev* 1998;7: 227–30.
42. Janakiram NB, Steele VE, Rao CV. Estrogen receptor-beta as a potential target for colon cancer prevention: chemoprevention of azoxymethane-induced colon carcinogenesis by raloxifene in F344 rats. *Cancer Prev Res* 2009;2:52–9.
43. Sato R, Suzuki T, Katayose Y, Miura K, Shiiba K, Tateno H, Miki Y, Akahira J, Kamogawa Y, Nagasaki S, Yamamoto K, Ii T, et al. Steroid sulfatase and estrogen sulfotransferase in colon carcinoma: regulators of intratumoral estrogen concentrations and potent prognostic factors. *Cancer Res* 2009;69:914–22.
44. Konstantinopoulos PA, Kominea A, Vandoros G, Sykiotis GP, Andricopoulos P, Varakis I, Sotiropoulou-Bonikou G, Papavassiliou AG. Oestrogen receptor beta (ERbeta) is abundantly expressed in normal colonic mucosa, but declines in colon adenocarcinoma paralleling the tumour's dedifferentiation. *Eur J Cancer* 2003;39:1251–8.
45. Jassam N, Bell SM, Speirs V, Quirke P. Loss of expression of oestrogen receptor beta in colon cancer and its association with Dukes' staging. *Oncol Rep* 2005;14: 17–21.
46. Castiglione F, Taddei A, Degl'Innocenti DR, Buccoliero AM, Bechi P, Garbini F, Chiara FG, Moncini D, Cavallina G, Marascio L, Freschi G, Gian LT. Expression of estrogen receptor beta in colon cancer progression. *Diagn Mol Pathol* 2008;17:231–36.
47. Fang YJ, Lu ZH, Wang F, Wu XJ, Li LR, Zhang LY, Pan ZZ, Wan DS. Prognostic impact of ERβ and MMP7 expression on overall survival in colon cancer. *Tumour Biol* 2010;31:651–8.

Journal of Pathology
J Pathol (2012)
Published online in Wiley Online Library
(wileyonlinelibrary.com) DOI: 10.1002/path.4019

ORIGINAL PAPER

Aromatase inhibitor treatment of breast cancer cells increases the expression of *let-7f*, a microRNA targeting *CYP19A1*

Yukiko Shibahara,[1] Yasuhiro Miki,[1] Yoshiaki Onodera,[1] Shuko Hata,[1] Monica SM Chan,[1,2–4] Christopher CP Yiu,[1,3] Tjing Y Loo,[1,2–4] Yasuhiro Nakamura,[1] Jun-ichi Akahira,[1] Takanori Ishida,[5] Keiko Abe,[1] Hisashi Hirakawa,[6] Louis WC Chow,[2–4,7] Takashi Suzuki,[1] Noriaki Ouchi[5] and Hironobu Sasano[1]*

[1] *Department of Pathology, Tohoku University Graduate School of Medicine, 2-1 Seiryo-machi, Aoba-ku, Sendai, Miyagi 980-8575, Japan*
[2] *UNIMED Medical Institute, Comprehensive Centre for Breast Diseases, 10/F, Luk Kwok Centre, 72 Gloucester Road, Wanchai, Hong Kong*
[3] *Department of Surgery, Li Ka Shing Faculty of Medicine, The University of Hong Kong, Queen Mary Hospital, 102 Pokfulam Road, Hong Kong*
[4] *Clinical Trial Centre, Li Ka Shing Faculty of Medicine, The University of Hong Kong, Queen Mary Hospital, 102 Pokfulam Road, Hong Kong*
[5] *Department of Surgery, Tohoku University Graduate School of Medicine, 2-1 Seiryo-machi, Aoba-ku, Sendai, Miyagi 980-8575, Japan*
[6] *Department of Surgery, Tohoku Kosai Hospital, 2-3-11 Kokubun-cho, Aoba-ku, Sendai, Miyagi 980-0803, Japan*
[7] *Organisation of Oncology and Translational Research, Unit A, 9/F, CNT Commercial Building, 302 Queen's Road Central, Hong Kong*

**Correspondence to: Hironobu Sasano, Department of Pathology, Tohoku University Graduate School of Medicine, 2-1 Seiryo-machi, Aoba-ku, Sendai, Miyagi 980-8575, Japan. e-mail: hsasano@patholo2.med.tohoku.ac.jp*

Abstract

Aromatase inhibitors (AIs) are considered the gold standard of endocrine therapy for oestrogen receptor-positive postmenopausal breast cancer patients. AI treatment was reported to result in marked alterations of genetic profiles in cancer tissues but its detailed molecular mechanisms have not been elucidated. Therefore, we profiled miRNA expression before and after treatment with letrozole in MCF-7 co-cultured with primary breast cancer stromal cells. Letrozole significantly altered the expression profiles of cancer miRNAs *in vitro*. Among the elevated miRNAs following letrozole treatment, computational analysis identified *let-7f*, a tumour-suppressor miRNA which targeted the *aromatase* gene (*CYP19A1*) expression. Quantitative real-time PCR assay using MCF-7 and SK-BR-3 cells as well as clinical specimens of a neoadjuvant study demonstrated a significant inverse correlation between *aromatase* mRNA and *let-7f* expression. In addition, high *let-7f* expression was significantly correlated with low aromatase protein levels evaluated by both immunohistochemistry and the western blotting method in breast cancer cases. Results of 3'UTR luciferase assay also demonstrated the actual *let-7f* binding sites in *CYP19A1*, indicating that *let-7f* directly targets the *aromatase* gene. Subsequent WST-8 and migration assays performed in *let-7f*-transfected MCF-7 and SK-BR-3 cells revealed a significant decrement of their proliferation and migration. These findings all demonstrated that *let-7f*, a tumour suppressor miRNA in breast cancer, directly targeted the *aromatase* gene and was restored by AI treatment. Therefore, AIs may exert tumour-suppressing effects upon breast cancer cells by suppressing *aromatase* gene expression via restoration of *let-7f*.

Keywords: aromatase inhibitors; *CYP19A1*; *let-7*; breast cancer

Received 24 October 2011; Revised 7 February 2012; Accepted 21 February 2012

Conflict of interest statement: HS received educational research grants from Novartis Japan Oncology and Pfizer Japan Oncology. YM received educational research grants from Pfizer Japan. The other authors disclosed no potential conflicts of interest.

Introduction

The treatment for oestrogen receptor-positive (ER+) postmenopausal breast cancer patients has advanced significantly in the past decades. Tamoxifen was considered the gold standard for endocrine therapy but the third-generation aromatase inhibitors (AIs) confer clinical benefits over tamoxifen in terms of decreased recurrence rates and increased relapse-free survival [1–4]. AIs are generally considered to work on ER+ breast cancer cells by depleting oestrogens through inhibiting the conversion of androgens to oestrogens, eliminating the pivotal sources of oestrogen necessary for tumour growth. Third-generation AIs include the non-steroidal inhibitor anastrozole and letrozole and the steroidal inhibitor exemestane. Both types of AIs have been extensively used in clinical practice but their detailed mechanisms have not been clarified.

Alterations in the protein-coding regions of genes following AI treatment have been reported, including genes associated with oestrogen regulation (*KIAA0101, ZWINT, IRS1*, and *TFF1*) and cell cycle progression (*CDK1, CCNB1*, and *CKS2*) in breast cancer cells [5]. In addition, Mackay *et al* reported that *aromatase* (*CYP19A1*) mRNA itself was significantly down-regulated by AIs [6]. microRNAs (miRNAs) are short non-protein coding RNAs known to play key regulatory roles in various cellular processes. Dysregulation

of miRNAs has been recently reported to play a key role in various therapeutic responses [7]. The equilibrium of miRNA expression is frequently disturbed in human cancers, with the miRNAs themselves acting as tumour suppressors or oncogenes [8]. miRNA profiling has led to the discovery of miRNAs that are aberrantly expressed in breast cancer including tumour suppressor miRNAs (*miR-206, miR-125, miR-17-5p, let-7, miR-34a*, and *miR-31*) and oncogenic miRNAs (*miR-21, miR-155, miR-10b*, and *miR-373/520c*) [9]. Widespread alterations of miRNA profiles by oestrogen administration have also been reported recently [10], which suggest a profound connection between oestrogen and tumour growth at the miRNA level.

We therefore performed miRNA PCR array using a third-generation AI, letrozole-treated breast cancer cell line to demonstrate the potential involvement of miRNAs in AI treatment. The results of this *in vitro* study revealed that letrozole treatment significantly altered the global expression profiles of miRNAs. Among tumour-suppressor miRNAs increased by letrozole treatment, computational analysis identified *let-7f* and its putative roles for directly targeting *CYP19A1* [11]. We further evaluated the correlation between aromatase expression and the status of *let-7f* in breast cancer cases and demonstrated an inverse correlation between *let-7f* and *aromatase* mRNA/protein expression. These results provide new insights into the roles of miRNAs in AI treatment of ER+ breast cancer patients.

Materials and methods

Chemicals

Letrozole was obtained from Novartis Pharma AG (Basel, Switzerland).

Cell lines and culture conditions

The human breast cancer cell lines MCF-7 and SK-BR-3 were provided by the Cell Resource Center for Biomedical Research, Tohoku University (Sendai, Japan). MCF-7 and SK-BR-3 cells were cultured in RPMI 1640 (Sigma-Aldrich, St Louis, MO, USA) and supplemented with 10% fetal bovine serum (FBS; Nichirei, Tokyo, Japan). Primary stromal cells employed in this study were provisionally designated 32N, isolated from operated breast cancer specimens using collagenase treatment [12], and maintained in RPMI 1640 with 10% FBS. MCF-7 and 32N were each cultured in RPMI 1640 with dextran-coated charcoal (DCC)–FBS for 3 days before each experiment to exhaust endogenous oestrogen.

Co-culture system and AI treatment

The co-culture method was employed in this study to induce *aromatase* mRNA expression in MCF-7 cells according to our previous reports [13]. This co-culture method was previously reported to induce aromatase through an interaction between stromal and breast cancer cells and has been considered useful for evaluating the effects of medications on breast cancer patients, mimicking their *in vivo* intratumoural microenvironment [13]. Transwell cultures were established in six-well plates or 100-mm dishes using ThinCert™ (0.4 μm pore; Greiner Bio-One, Germany) in order to promote physical separation of the stromal and carcinoma cell lines. MCF-7 cells were cultured in transwell chambers in the absence or presence of 32N cells and were cultivated on the bottom of the plates or dishes (MCF-7co). After 48 h of cultivation using this co-culture system, letrozole (10^{-8} mol/l) was applied for 48 h (MCF-7co/le). MCF-7 and 32N cells were separated and total RNA was isolated from three samples each for MCF-7, MCF-7co, and MCF-7co/le using the TRIzol method according to the manufacturer's instructions. SK-BR-3 cells were not co-cultured with stromal cells because SK-BR-3 was known to express relatively strong aromatase activity, according to a previous report [13].

Patients and tissue collection

Three frozen breast cancer tissue specimens from ER+, postmenopausal patients receiving neoadjuvant AI treatment (3 months of letrozole, 2.5 mg daily) were obtained from the Celecoxib Anti-Aromatase Neoadjuvant Trial (CAAN Trial) [14], a clinical trial conducted at The University of Hong Kong and Queen Mary Hospital, Hong Kong. Eleven frozen ER+ breast cancer tissue samples used for real-time PCR and nine frozen breast cancer tissue samples used for western blotting, which did not receive any prior treatment, were obtained from Tohoku University Hospital, Sendai, Japan. Informed consent was obtained from all patients. The research protocol for this study was approved by the Ethics Committee at The University of Hong Kong (HK1821-02) and Tohoku University School of Medicine (2010-509). Prior to RNA extraction, the frozen sections were stained with haematoxylin and eosin for detailed histological evaluation under light microscopy. Briefly, the entire frozen tissues were disrupted using a tissue homogenizer and total RNA including miRNA was extracted using TRIzol Reagent (Invitrogen, Carlsbad, CA, USA).

Laser capture microdissection (LCM) in 10% formalin-fixed, paraffin-embedded (FFPE) tissues

Twenty FFPE breast cancer tissues retrieved from the surgical pathology files of Tohoku Kosai Hospital were sectioned at a thickness of 8 μm. Carcinoma components were subsequently laser-transferred with care under light microscopic evaluation. LCM was performed using mmi CellCut (Molecular Machines & Industries AG, Glattbrug, Switzerland). MiRNA was extracted using a PureLink miRNA Isolation Kit (Invitrogen). cDNA was also synthesized using an RT^2 miRNA First Strand kit (Qiagen, Hilden, Germany). Research protocols for this study were approved by the

Ethics Committee at both Tohohu Kosai Hospital (No H17.8.5) and Tohoku University School of Medicine (2009-203), respectively.

Transfection

Hsa-let-7f (Genolution Pharmaceuticals, Seoul, Korea) was transfected into MCF-7 cells by Lipofectamine 2000 (Invitrogen) with 5 or 10 nM mature microRNA molecules for 24, 48, and 72 h. Scramble siRNA (Genolution Pharmaceuticals) was used as a negative control.

Quantitative reverse transcription real-time PCR of *aromatase* mRNA

For real-time PCR on the expression of *aromatase* mRNA in MCF-7, SK-BR-3, and clinical samples, total RNA was extracted as described above. cDNA was synthesized using a QuantiTect reverse transcription kit (Qiagen). Real-time PCR was carried out using the LightCycler System and FastStart DNA Master SYBR Green I (Roche Diagnostics, Mannheim, Germany). The PCR primer sequences used in this study were as follows: *aromatase* (X13 589), forward 691–reverse 806; and the *ribosomal protein L13a* (*RPL13A*) (NM_012 423), forward 487–reverse 612 [13]. cDNA of known *aromatase* concentration and the housekeeping gene *RPL13A* were used to generate standard curves for real-time quantitative PCR in order to determine the quantity of target cDNA transcript. The mRNA level in each case was represented as a ratio of *RLP13A*.

Quantitative reverse transcription real-time PCR of miRNA

For cancer-related miRNA profiling in MCF-7 cells, total RNA was extracted as described above. MCF-7co and MCF-7co/le were analysed for the expression of a panel of 88 cancer-related miRNAs using RT^2 miRNA PCR Array Human Cancer MAH-102A (Qiagen). For *let-7f* quantification in MCF-7 and SK-BR-3 cells, frozen breast cancer tissues and FFPE specimens, total RNA or miRNA was extracted as described above and quantified using RT^2 miRNA qPCR assay (Qiagen). *U6* was used for normalization; conditions employing no templates and/or reverse transcription were included as negative controls. PCR was performed on an ABI7500 Real-Time PCR System (Applied Systems, Foster City, CA, USA). Data analysis was performed with the web-based software package for the miRNA PCR array system (http://www.sabiosciences.com/pcr/arrayanalysis.php).

Target prediction of miRNA

TargetScan 5.1 (http://www.targetscan.org/), MiRanda (http://www.microrna.org/), PicTar (http://pictar.mdc-berlin.de/), and PITA (http://genie.weizmann.ac.il/pubs/mir07/mir07_notes.html) were used to search for putative targets of miRNAs that were altered by letrozole treatment and also for miRNAs which target *aromatase*.

Immunohistochemistry

The antibodies used in this study were as follows: ERα (ER1D5; Immunotech SA, Marseilles, France); progesterone receptor (MAB429; Chemicon International Inc, Temecula, CA, USA); Ki-67 (MIB1; DakoCytomation Co Ltd, Kyoto, Japan); and aromatase [13]. For aromatase, the approximate percentage of cells staining (proportion score) was classified into the following four groups: 0, < 1%; 1, 1–25%; 2, 26–50%; and 3, >50% immuno-positive cells. The relative immuno-intensity of aromatase positive cells was classified as follows: 0, no immunoreactivity; 1, weak; 2, moderate; and 3, intense immunoreactivity. Aromatase immunoreactivity was evaluated as a total score composed of the proportion score plus the relative immuno-intensity score [13].

Western blotting

Nine frozen breast cancer tissue samples were available for western blotting. Tissue protein was extracted using M-PER Mammalian Protein Extraction Reagent (Pierce Biotechnology, Rockford, IL, USA) with Halt Protease Inhibitor Cocktail (Pierce Biotechnology). Following SDS-PAGE (10% acrylamide gel), proteins were transferred onto Hybond P polyvinylidene difluoride membrane (GE Healthcare, Buckinghamshire, UK). The primary antibodies used in this study were aromatase [13] and β-actin (AC-15; Sigma-Aldrich). Antibody–protein complexes on the blots were detected using ECL Plus western blotting detection reagents (GE Healthcare). The protein bands were visualized and the immuno-intensity of specific bands was quantified using an LAS-1000 image analyzer (Fuji Photo Film Co, Tokyo, Japan). The relative immuno-intensity of aromatase was evaluated as a ratio of β - actin in each sample examined in our study.

Luciferase reporter assay

A pmirGLO Dual-Luciferase miR Target Expression Vector was used for 3'UTR luciferase assays (Promega Corporation, Madison, WI, USA). The following primer sequences were used: *CYP19A1* forward primers, F1 (5′-AAAGCTAGCCTAGAGAAGGCTGG TCAGTAC-3′) and F2 (5′-AAAGCTAGCTAAAGAA CGTGGTCAGAGTAG-3′); *CYP19A1* reverse primers, R1 (5'AAACTCGAGGTTAAATCTCTCAGGTAACT G-3′) and R2 (5′-AAACTCGAGCTCTGACCACGT TCTTTACTG-3′) (Figures 4a and 4b). The annealed oligonucleotides were ligated into the XhoI/NheI site of pmirGLO Dual-Luciferase miR Target Expression Vector. The constructs were then verified by sequencing. MCF-7 cells were co-transfected with 5 nM scramble siRNA or *hsa-let-7f* (Genolution Pharmaceuticals) and 5 ng of pmirGLO Dual-Luciferase miRNA Target

Expression Vectors using Lipofectamine 2000 (Invitrogen). Vectors containing the target sequence were amplified using F2 and R1 (92 base pairs) and F1 and R2 (1164 base pairs) (named pGL-V1 and pGL-V2, respectively); vectors not containing the target sequence were amplified using F1 and R2 (1100 base pairs) (named pGL-V3). The DNA sequences of these three constructs were confirmed by DNA sequencing. Luciferase assay was performed using the Dual-Luciferase Reporter Assay System (Promega) at 24 h following the transfection according to the manufacturer's protocols. Firefly luciferase activity was normalized to Renilla luciferase activity.

Cell proliferation assay

MCF-7 and SK-BR-3 cells were each cultured in low-adhesion 24-well plates (AGC Techno Glass Co, Ltd, Chiba, Japan) and transfected with *let-7f* (5, 10, and 50 nM). Cell proliferation was measured using the WST-8 colorimetric assay (Cell Counting Kit-8; Dojindo Laboratories, Kumamoto, Japan [15]). Briefly, WST-8 reagent solution was added to each well, after which the microplates were incubated for 2 h at 37 °C. The absorbance at 450 nm was then measured using a cell counter (Sysmex CDA-500, Sysmex Corporation, Hyogo, Japan).

Wound healing assay

Cell migration was analysed using a modified wound healing assay. Briefly, the wound healing assay was performed using ibidi Culture-Insert (ibidi GmbH, Munich, Germany) inserted in 24-well plates. After the cells became confluent, a cell-free gap of 500 μm was created by removing the Culture-Insert. Cells migrating into the gap region were observed by microscopy and we took photographs of the cell-free gap areas of three different fields using an Olympus digital camera.

Statistical analysis

All statistical analyses were performed using StatView (USA). A p value of less than 0.05 was regarded as statistically significant.

Results

Effects of letrozole treatment on *aromatase* mRNA expression in breast cancer cell lines

Co-culture of MCF-7 with stromal cells significantly increased *aromatase* mRNA levels, which is consistent with the results of our previously reported study [13]. Forty-eight hours of letrozole treatment resulted in a significant decrease of *aromatase* mRNA in MCF-7 (control MCF-7co = 0.00082 ± 0.0001646; MCF-7co/le: 6 h = 0.000671 ± 0.0000222, 12 h = 0.000837 ± 0.0001793, 24 h = 0.00077 ± 0.0000557 ± ?, 48 h = 0.00034 ± 0.00005*, *$p < 0.05$) (Figure 1a). Forty-eight hours of letrozole treatment in SK-BR-3 also resulted in a 23.9% decrease of *aromatase* mRNA (data not shown).

Alterations of microRNA profiles following letrozole treatment in breast cancer cell lines

Results of the PCR array in letrozole-treated MCF-7 cells demonstrated that five miRNAs were down-regulated and 13 miRNAs were up-regulated by more than two-fold (Figure 1b). These miRNAs were further analysed for possible targeting of the *aromatase* gene (*CYP19A1*) using the multiple prediction programs described above. From this analysis, *let-7f* was calculated to contain the optimum sequence for directly targeting *CYP19A1*. Therefore, we subsequently focused on *let-7f*. Significant up-regulation of *let-7f* by 48 h of letrozole treatment in MCF-7 cells as well as SK-BR-3 cells was confirmed by the RT^2 miRNA qPCR assay ($p < 0.05$, Figure 1c). We also performed qRT-PCR in paired breast cancer cases receiving neoadjuvant letrozole treatment in order to verify these findings in clinical cases. Two out of three cases demonstrated marked up-regulation of *let-7f* (Figure 2).

Relationship between *let-7f* and aromatase expression levels in breast cancer tissues

The results of multiple target prediction algorithms revealed that *let-7f* negatively regulated *aromatase* gene expression. We then examined the possible correlation between *aromatase* mRNA and *let-7f* expression from 11 frozen breast cancer tissues. Elevated *aromatase* mRNA expression was significantly associated with low *let-7f* expression in these cases (Figure 3a, $p < 0.05$).

For examination of the correlation between *let-7f* and aromatase protein, immunohistochemistry and western blotting were utilized. The amount of *let-7f* expression in breast cancer cells isolated by laser capture microdissection was compared with that of immunohistochemical aromatase reactivity in 20 cases. Higher *let-7f* expression was significantly associated with a lower total score of aromatase immunoreactivity (Figures 3b and 3c, $p < 0.05$). The results of western blotting also indicated that *let-7f* expression and aromatase protein levels were inversely correlated (Figure 3d, $Y = 0.965 - 0.386 \times X$, $R^2 = 0.275$, $p = 0.0255$). These findings all demonstrate an inverse correlation between the expression of *let-7f* and aromatase in breast cancer.

Correlation between *let-7f* and *CYP19A1* in breast cancer cells

Transient transfection of pGL-V1 and pGL-V2 (target sequence included) in the presence of *let-7f* resulted in a significant decrease of luciferase activity compared with that of scramble siRNA but transfection of pGL-V3 (target sequence not included) did not result in a significant loss of luciferase activity (Figure 4). These results confirmed the role of *let-7f* in regulating

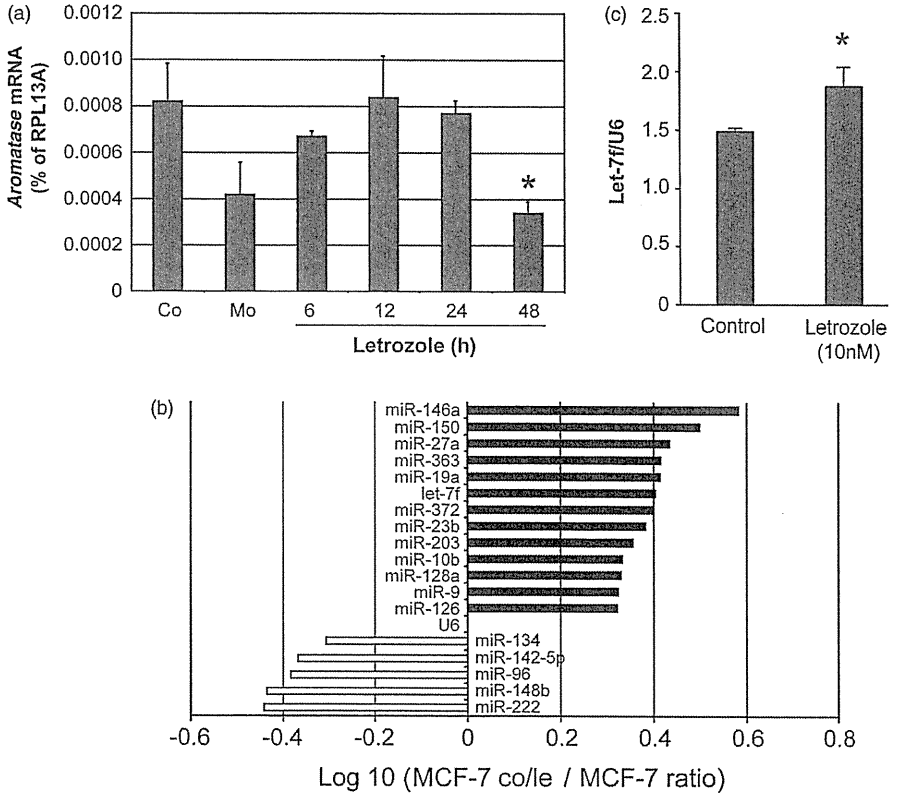

Figure 1. (a) *Aromatase* mRNA expression of MCF-7 was up-regulated by co-culture with primary stromal cells obtained from human breast cancer tissues and down-regulated by subsequent letrozole treatment. Values for *aromatase* mRNA are depicted as per cent expression to *RPL13A* by quantitative RT-PCR. MCF-7 cells were co-cultured with stromal cells for 48 h. Stromal cells were then removed and MCF-7 cells received 6, 12, 24 or 48 h of AI treatment. $^*p < 0.05$ versus MCF-7co. This experiment was independently performed in triplicate. (b) MiRNAs which were up-regulated or down-regulated by letrozole treatment relative to MCF-7/co by more than two-fold were included. Values of miRNAs were normalized to *U6*. The miRNAs were ranked according to the fold changes. This experiment was performed twice independently. (c) *Let-7f* expression was up-regulated by 48 h of letrozole treatment in SK-BR-3 cells. Values for *let-7f* were normalized to *U6*. This experiment was independently performed in triplicate.

CYP19A1 expression by actual binding to the target sequence within the 3'UTR of *CYP19A1*.

The effects of *let-7f* miRNA on *in vitro* proliferation and migration of MCF-7 and SK-BR-3 cells

The level of *let-7f* expression was significantly increased following *let-7f* transfection (data not shown). At 24 h post-transfection, the densities of the MCF-7 cells transfected with 50 nM *let-7f* were significantly lower than those of the cells transfected with scramble siRNA (control miRNA = 0.615 ± 0.057, *let-7f* = 0.2313 ± 0.027, $^*p < 0.05$, relative levels). At 48 and 72 h, the results of the WST-8 assays demonstrated significantly lower cell numbers in MCF-7 cells treated with 5, 10, and 50 nM *let-7f* compared with scramble siRNA-transfected MCF-7 cells [48 h: control miRNA = 1.109 ± 0.096, *let-7f* (5 nM) = 0.722 ± 0.055*, *let-7f* (10 nM) = 0.286 ± 0.019*, *let-7f* (50 nM) = 0.118 ± 0.008*; 72 h: control miRNA = 1.680 ± 0.126, *let-7f* (5 nM) = 0.599 ± 0.166*, *let-7f* (10 nM) = 0.136 ± 0.016, *let-7f* (50 nM) = 0.099 ± 0.011*; $^*p < 0.05$, relative levels] (Figures 5a–5c). The densities of SK-BR-3 cells transfected with 10 nM *let-7f* were also significantly decreased compared with those of the control group at 48 h (Figure 5d) [control miRNA = 0.563 ± 0.026, *let-7f* (5 nM) = 0.501 ± 0.011, *let-7f* (10 nM) = 0.463 ± 0.027*; $^*p < 0.05$].

In the wound healing assay, at 48–72 h following the gap creation, *let-7f* transfection resulted in a significant decrease of cellular migration into the gap regions in MCF-7 cells, which widened the cell-free gap by 18.5%* and 29.6%* at 10 nM, 48 and 72 h, respectively, compared with miR-control transfected cells ($^*p < 0.05$) (Figures 6a–6c). SK-BR-3 cells were slower growing compared with MCF-7 cells but *let-7f* transfection for 96 h significantly inhibited cell migration and widened the cell-free gap by 13.6%* and 11.4%* at 5 and 10 nM, respectively, compared with the control group ($^*p < 0.05$) (Figure 6d).

Discussion

We have shown that AI treatment can increase the expression of tumour-suppressing miRNAs. This interaction is important as miRNAs constitute a novel gene target network by regulating the expression of several hundred target genes, including important oncogenes

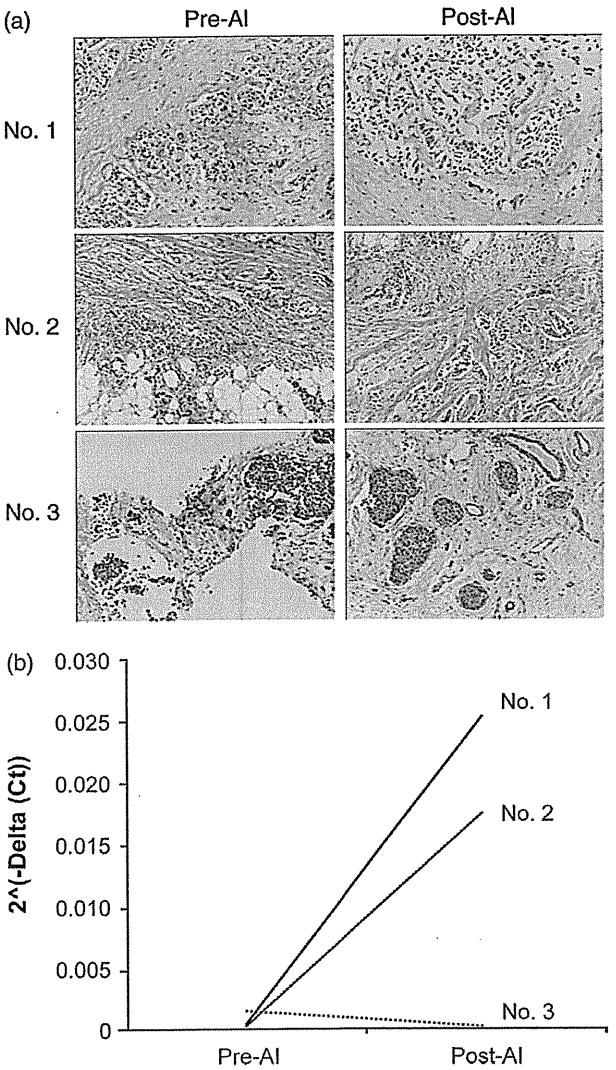

Figure 2. RT-PCR analysis of *let-7f* expression alterations in paired breast cancer specimens receiving 3 months of neoadjuvant AI treatment. (a) Representative presentation of haematoxylin and eosin staining of specimens 1–3; pre-AI (left) and post-AI (right). (b) Individual changes of *let-7f* expression by letrozole treatment were summarized. Restoration of *let-7f* was detected in two out of three cases receiving letrozole treatment. *U6* probe was used for normalization of expression levels.

and tumour suppressors [8,16,17]. Therefore, an analysis of miRNA profile alterations following AI treatment will contribute to the elucidation of its molecular mechanisms. However, few studies have reported the potential involvement of miRNA in the treatment of AIs [18,19]. Masri *et al* reported that *miR-128a* was up-regulated in letrozole-resistant breast cancer cell lines [18,19] but they studied only breast cancer cells resistant to AI. Maillot *et al* [10] reported miRNA profiling in breast cancer specimens treated by tamoxifen combined with exemestane. Therefore, our present study is the first one to demonstrate alterations of miRNA expression as a result of only AI treatment in breast cancer cells.

Genetic changes occur at the mRNA level with AI treatment as Mackay *et al* recently reported that the *aromatase* mRNA itself was down-regulated by AI treatment in breast cancer cells [6]; however, the mechanism for this phenomenon is unknown. We hypothesized that the reason for this finding may be due to the alterations of the miRNA profile caused by AI treatment. To verify this hypothesis, we performed a miRNA PCR array on a letrozole-treated breast cancer cell line. Several miRNAs were altered by letrozole treatment and among these miRNAs, we specifically detected the restoration of *let-7f*, a tumour-suppressor miRNA. The *let-7* family, to which *let-7f* belongs, is suppressed in various human malignancies [20], and its restoration to normal levels has been reported to suppress cancer growth [21–23]. In our present study, *let-7f* was also demonstrated to suppress cell proliferation and migration *in vitro*. These findings are supported by the recent results by Yu *et al*, who showed that *let-7* overexpression resulted in decreased breast tumour-initiating cells (BT-ICs) [24], and Zhao *et al*, who recently demonstrated decreased cell proliferation by *let-7b* and *let-7i* in breast cancer cells [25]. It then became important to evaluate whether these alterations occur *in vivo*. We therefore evaluated the changes of *let-7f* in patients who received neoadjuvant letrozole therapy and correlated the changes of *let-7f* with therapeutic response; Ki-67 (MIB-1 labelling index) was used as a marker of therapeutic efficacy [26]. Two out of three cases which showed increased levels of *let-7f* expression resulted in a marked decrease of Ki-67 (%) following letrozole treatment. The remaining case did not show any change in Ki-67 (%) as this case showed a very low Ki-67 index initially (Supporting information, Supplementary Figure 1). Although the number of clinical cases studied in our study was too small to draw any conclusions, these results suggest that the actions of letrozole on the *aromatase* gene via *let-7f* restoration may be contributing to oestrogen depletion and decreased tumour cell proliferation effects of AIs. Moreover, this may explain the improved relapse and recurrence rates with AI treatment in ER+ breast cancer patients. Further investigations including the study of more patients undergoing neoadjuvant therapy are required for clarification of this interesting hypothesis.

We hypothesized that the *aromatase* gene would be directly targeted by *let-7f*. This was subsequently verified by our experiments. First, an increased level of *let-7f* was detected as a result of letrozole treatment, while the levels of *aromatase* mRNA were decreased in these breast cancer cells. Second, *let-7f* expression was negatively correlated with the level of *aromatase* mRNA expression in both MCF-7 cells and breast cancer tissues. Third, a significant inverse correlation was detected between *let-7f* and aromatase protein expression in FFPE and frozen breast cancer tissues by immunohistochemistry and western blotting. miRNA is preserved excellently in FFPE tissues; therefore they were used in this study [27]. Fourth, transfection of *let-7f* decreased the activities of the luciferase reporter containing the 3'UTR sequence of the *CYP19A1* gene. These results all indicated that

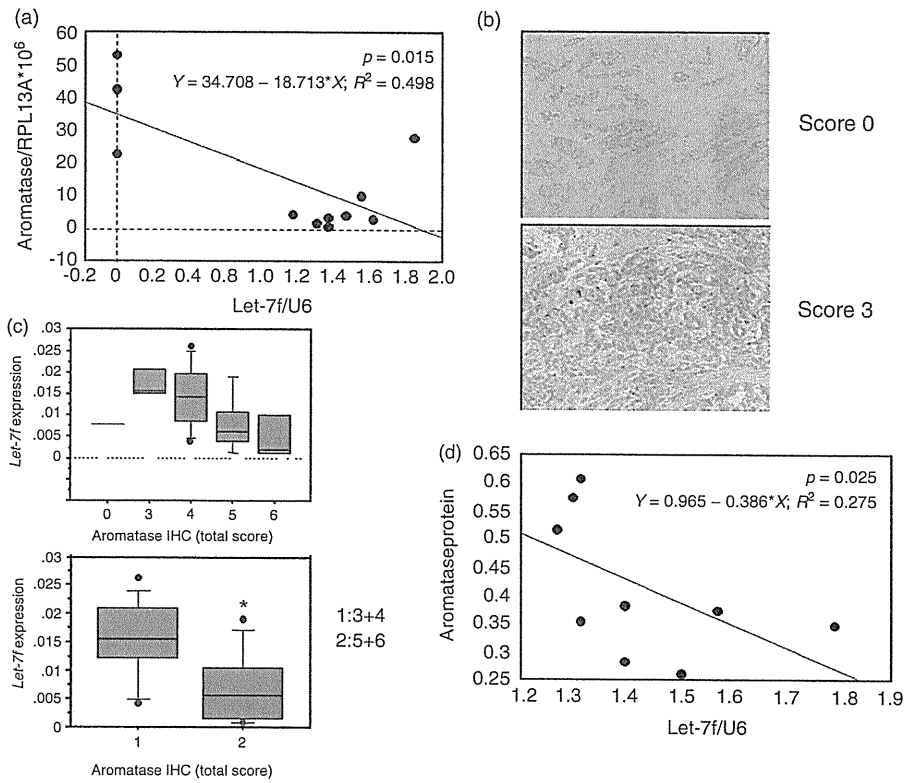

Figure 3. (a) Inverse correlation between *aromatase* mRNA expression and *let-7f* in clinical cases. *Aromatase* mRNA expression was demonstrated as a fraction of *RPL13A* by quantitative RT-PCR. *Let-7f* expression was examined using qRT-PCR and normalized to *U6* probe. (b) Relative immuno-intensity of aromatase positive cells was demonstrated: 0, no immunoreactivity, to 3, intense immunoreactivity. (c) Aromatase immunoreactivity was evaluated as a total score = proportion score + relative immuno-intensity score [13]. Expression of *let-7f* in breast cancer cells was evaluated using LCM and qRT-PCR and subsequently compared with aromatase immunoreactivity. *Let-7f* expression was negatively correlated with aromatase immunoreactivity. $*p < 0.05$. See the Materials and methods section for details. (d) Expression of *let-7f* in frozen breast cancer specimens was evaluated by qRT-PCR and compared with the aromatase protein level using western blotting. Immuno-intensity of aromatase was quantified using an LAS-1000 image analyser and evaluated as a ratio of b-actin in each sample.

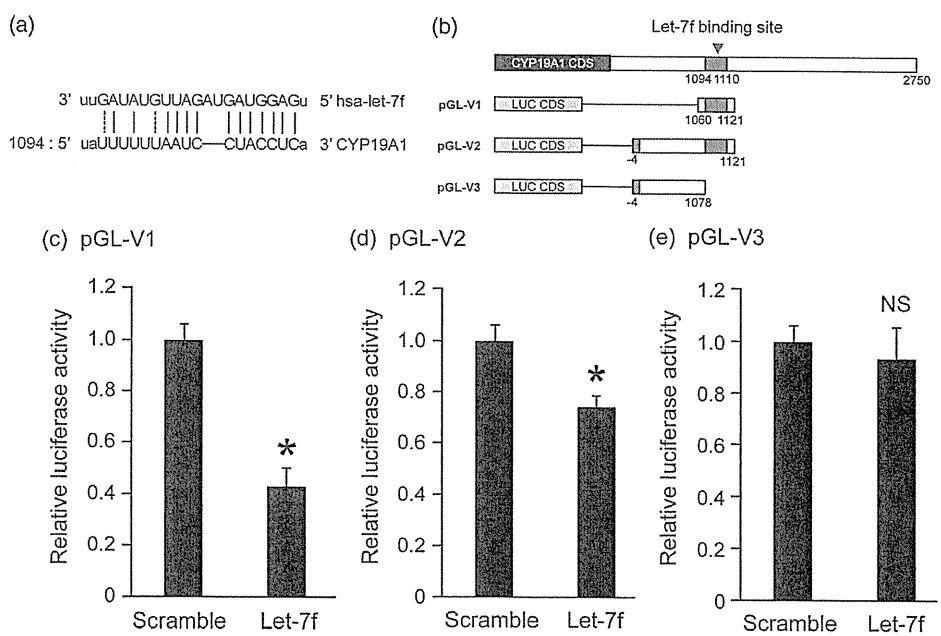

Figure 4. *Let-7f* directly targeted the *aromatase* gene (*CYP19A1*). (a) *Let-7f* target prediction: 3'UTR base pairing between *let-7f* and *CYP19A1*. *Hsa-let-7f/CYP19A1* alignment provided by http://www.microrna.org/. (b) Constructs of the vector, pGL-V1, -V2, and -V3, are demonstrated. *Let-7f* significantly inhibited luciferase activity with (c) pGL-V1 and (d) pGL-V2, which included the *CYP19A1* binding site within 3'UTR. (e) Luciferase activity was not inhibited when pGL-V3, which did not include the binding site, was inserted. $*p < 0.05$ versus scramble siRNA. NS = not significant. All experiments were performed in triplicate independently.

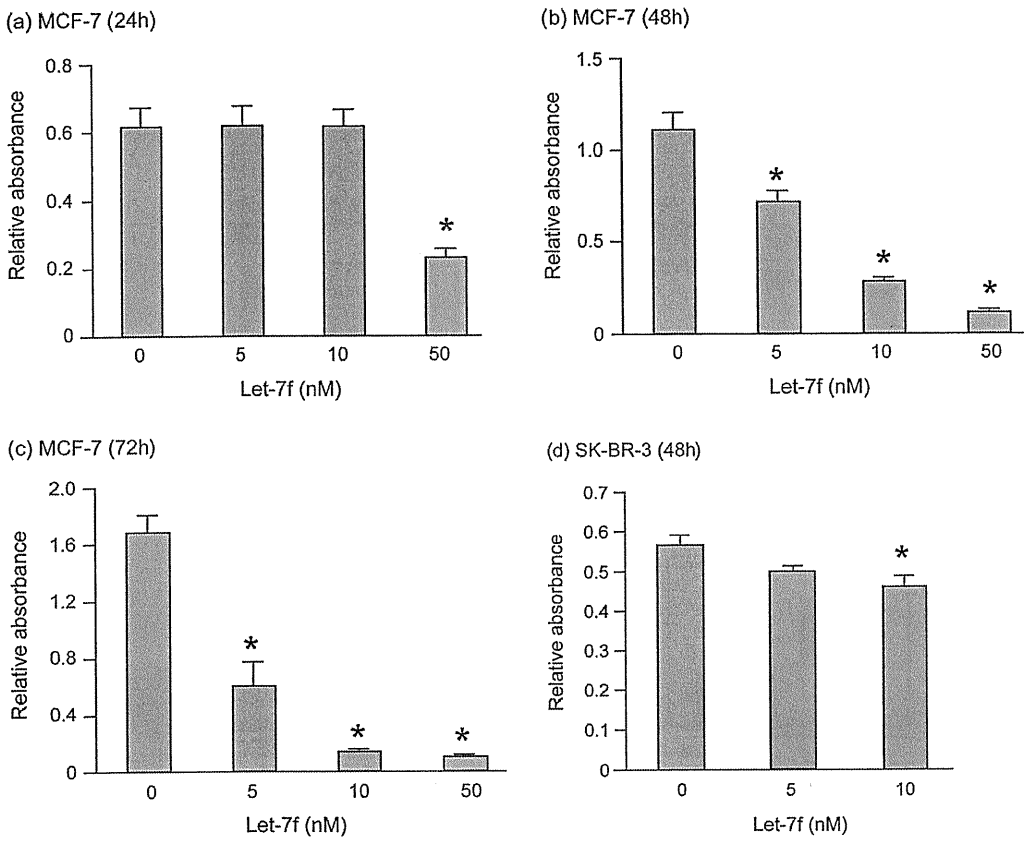

Figure 5. Effects of *let-7f* on cell proliferation in MCF-7 (a–c) and SK-BR-3 (d) cell lines using the WST-8 assay. $*p < 0.05$ compared with scramble siRNA. MCF-7: (a) 24 h, (b) 48 h, and (c) 72 h; and SK-BR-3: (d) 48 h after transfection. Cell proliferation was strongly inhibited by *let-7f*.

CYP19A1 was negatively regulated by *let-7f* in its expression. This may also explain why the *aromatase* gene itself is suppressed by AI treatment via translational suppression by *let-7f*.

We present here two theories which may explain the mechanism of *let-7f* up-regulation by letrozole. The first theory is that *let-7f* restoration by letrozole may be a secondary phenomenon following oestrogen withdrawal and tumour inhibition by AI. Genetic changes by AI were reported earlier at the mRNA level by Mackay *et al*, who showed that many oestrogen-regulated genes were secondarily altered by AI treatment [6]. At the miRNA level, our results as well as previous reports demonstrate that *let-7* is a multifunctional miRNA possessing tumour-suppressing effects as well as oestrogen-regulating features [10]. Therefore, *let-7* up-regulation may simply be a manifestation of the secondary genetic changes that occurred in the tumour environment by AI. The second theory is that letrozole may primarily and directly influence the miRNA expression profiles of cancer cells; therefore, the tumour-inhibiting properties of letrozole are due to *let-7* restoration by letrozole. The extent of our study is too limited to explain whether this possible direct interaction of cancer cells and letrozole is due to the unique molecular structure of letrozole or other mechanisms. Studies of letrozole-treated cases linked with clinical outcome should clarify this.

There is increasing evidence suggesting the importance of miRNAs in modulating sensitivity and resistance to therapy in various human malignancies [7]. For instance, the suppression of *miR-21* was reported to sensitize MCF-7 cells to the anti-cancer agent topotecan [28]. Similar studies have been reported in the case of tamoxifen [29] and have highlighted the importance of miRNAs in endocrine therapy as well as conventional chemotherapy. Resistance to AIs is currently a major clinical problem in AI therapy and many approaches to address this have been reported in the literature. The results of our present study and a previous report by Garcia-Casado *et al* imply the importance of the 3'UTR region of *CYP19A1* in relation to AI resistance [30]. Garcia-Casado *et al* reported that cases showing polymorphisms of rs4646 in the 3'UTR of the *CYP19A1* gene presented with a poor clinical response to letrozole and short progression-free survival [30]. Data from our study confirmed the actual *let-7f* binding region among the 3'UTR of *CYP19A1*. Taken together, these data point to the possibility that genetic alteration in the 3'UTR region leads to either the inability of *let-7f* to bind to *CYP19A1* or a less efficient rate of *CYP19A1* translation inhibition. This would result in weaker tumour-suppressing properties for letrozole. Our study is of clinical significance in this way as genetic alterations in the 3'UTR region of *CYP19A1* may be the key to explaining AI resistance.

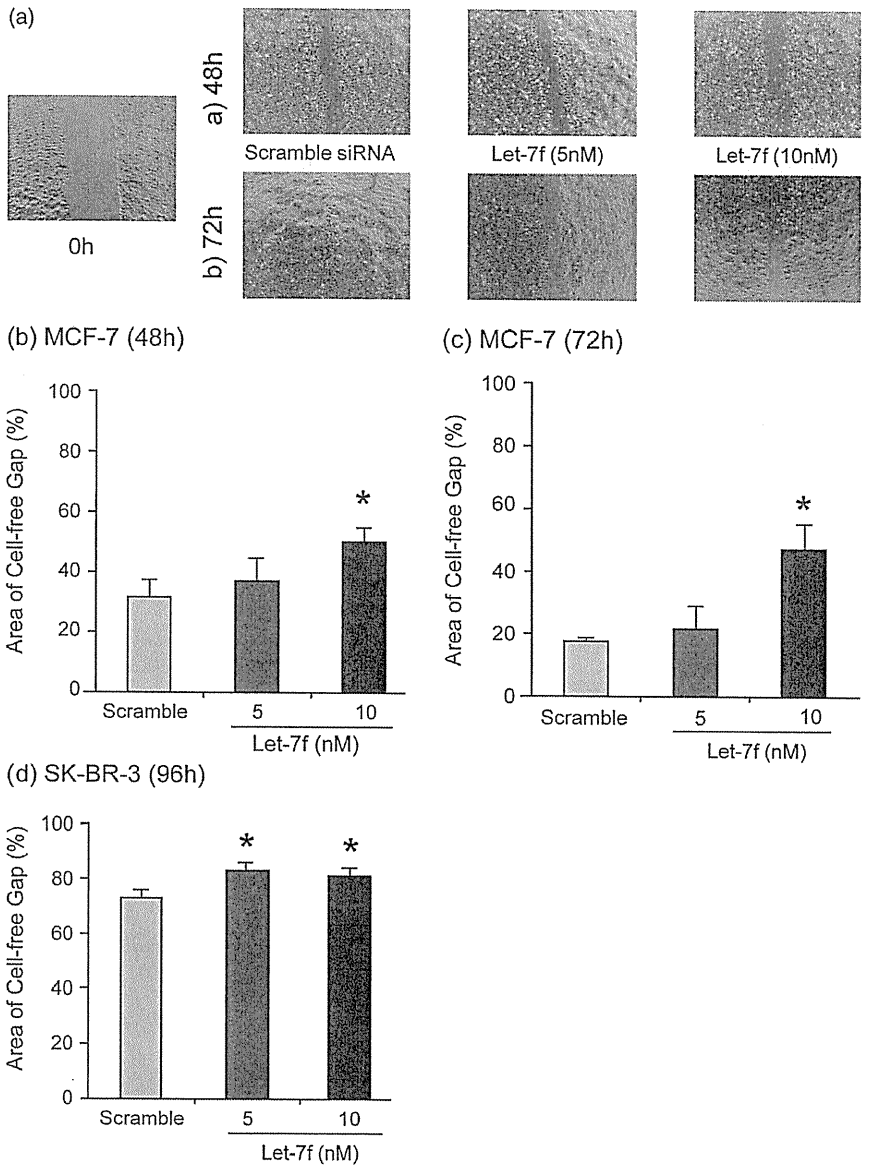

Figure 6. Effects of *let-7f* on cell migration in MCF-7 (a–c) and SK-BR-3 (d) cell lines using a modified wound healing assay. (a) Representative illustration of MCF-7. (b, c) *Let-7f* transfection reduced the area of the cell-free gap after 48 and 72 h in MCF-7. (d) *Let-7f* transfection reduced the area of the cell-free gap after 96 h in SK-BR-3 compared with scramble siRNA transfection. $^*p < 0.05$ versus scramble siRNA.

In conclusion, we firstly demonstrated that *let-7f* expression was up-regulated by AI treatment in both breast cancer cells and clinical specimens, which resulted in decreased cell proliferation of breast cancer cells. The results of our study also revealed that *let-7f* directly targeted *aromatase* gene expression. These results raise the possibility that *let-7* restoration accounts for the tumour-suppressing effects of AI through its actions on *aromatase* mRNA expression.

Acknowledgment

We thank Katsuhiko Ono and Ikumi Miura (Department of Pathology, Tohoku University School of Medicine, Sendai, Japan) for skilful technical assistance. We are grateful to Keely Mcnamara for assistance with technical English editing.

Author contribution statement

YS and YM conceived and designed the study. YS performed most of the experiments and drafted the manuscript. MSMC, CCPY, TYL, LWCC, TI, HH, and NO collected and stored all the samples. YO, SH, and YM contributed in immunohistochemistry and *in vitro* analyses. TS, KA, JA, and YN performed data analysis and histopathological correlations. HS supervised all experiments. YM and HS edited the manuscript. All authors read and approved the final manuscript.

References

1. Joerger M, Thurlimann B. Update of the BIG 1–98 Trial: where do we stand? *Breast* 2009; **Suppl 3**: S78–S82.

2. Josefsson ML, Leinster SJ. Aromatase inhibitors versus tamoxifen as adjuvant hormonal therapy for oestrogen sensitive early breast cancer in post-menopausal women: meta-analyses of monotherapy, sequenced therapy and extended therapy. *Breast* 2010; **19**: 76–83.
3. Coombes RC, Kilburn LS, Snowdon CF, *et al*. Survival and safety of exemestane versus tamoxifen after 2–3 years' tamoxifen treatment (Intergroup Exemestane Study): a randomised controlled trial. *Lancet* 2007; **369**: 559–570.
4. BIG 1–98 Collaborative Group, Mouridsen H, Giobbie-Hurder A, Goldhirsch A, *et al*. Letrozole therapy alone or in sequence with tamoxifen in women with breast cancer. *N Engl J Med* 2009; **361**: 766–776.
5. Miller WR. Clinical, pathological, proliferative and molecular responses associated with neoadjuvant aromatase inhibitor treatment in breast cancer. *J Steroid Biochem Mol Biol* 2010; **118**: 273–276.
6. Mackay A, Urruticoechea A, Dixon JM, *et al*. Molecular response to aromatase inhibitor treatment in primary breast cancer. *Breast Cancer Res* 2007; **9**: R37.
7. Blower PE, Verducci JS, Lin S, *et al*. MicroRNA expression profiles for the NCI-60 cancer cell panel. *Mol Cancer Ther* 2007; **6**: 1483–1491.
8. Zhang B, Pan X, Cobb GP, *et al*. MicroRNAs as oncogenes and tumor suppressors. *Dev Biol* 2007; **302**: 1–12.
9. O'Day E, Lal A. MicroRNAs and their target gene networks in breast cancer. *Breast Cancer Res* 2010; **12**: 201.
10. Maillot G, Lacroix-Triki M, Pierredon S, *et al*. Widespread estrogen-dependent repression of microRNAs involved in breast tumor cell growth. *Cancer Res* 2009; **69**: 8332–8340.
11. Barh D, Parida S, Parida B, *et al*. Let-7, miR-125, miR-205, and miR-296 are prospective therapeutic agents in breast cancer molecular medicine. *Gene Ther Mol Biol* 2008; **12**: 189–206.
12. Yamaguchi Y, Takei H, Suemasu K, *et al*. Tumor–stromal interaction through the estrogen-signaling pathway in human breast cancer. *Cancer Res* 2005; **65**: 4653–4662.
13. Miki Y, Suzuki T, Tazawa C, *et al*. Aromatase localization in human breast cancer tissues: possible interactions between intratumoral stromal and parenchymal cells. *Cancer Res* 2007; **67**: 3945–3954.
14. Chow LW, Yip AY, Loo WT, *et al*. Celecoxib anti-aromatase neoadjuvant (CAAN) trial for locally advanced breast cancer. *J Steroid Biochem Mol Biol* 2008; **111**: 13–17.
15. Isobe I, Michikawa M, Yanagisawa K. Enhancement of MTT, a tetrazolium salt, exocytosis by amyloid beta-protein and chloroquine in cultured rat astrocytes. *Neurosci Lett* 2007; **266**: 129–132.
16. Cowland JB, Hother C, Gronbaek K. MicroRNAs and cancer. *APMIS* 2007; **115**: 1090–1106.
17. Iorio MV, Croce CM. MicroRNAs in cancer: small molecules with a huge impact. *J Clin Oncol* 2009; **27**: 5848–5856.
18. Masri S, Liu Z, Phung S, *et al*. The role of microRNA-128a in regulating TGFbeta signaling in letrozole-resistant breast cancer cells. *Breast Cancer Res Treat* 2010; **124**: 89–99.
19. Masri S, Phung S, Wang X, *et al*. Molecular characterization of aromatase inhibitor-resistant, tamoxifen-resistant and LTEDaro cell lines. *J Steroid Biochem Mol Biol* 2010; **118**: 277–282.
20. Jerome T, Laurie P, Louis B, *et al*. Enjoy the silence: the story of let-7 microRNA and cancer. *Curr Genomics* 2007; **8**: 229–233.
21. Takamizawa J, Konishi H, Yanagisawa K, *et al*. Reduced expression of the let-7 microRNAs in human lung cancers in association with shortened postoperative survival. *Cancer Res* 2004; **64**: 3753–3756.
22. Kumar MS, Erkeland SJ, Pester RE, *et al*. Suppression of non-small cell lung tumor development by the let-7 microRNA family. *Proc Natl Acad Sci U S A* 2008; **105**: 3903–3908.
23. Akao Y, Nakagawa Y, Naoe T. let-7 microRNA functions as a potential growth suppressor in human colon cancer cells. *Biol Pharm Bull* 2006; **29**: 903–906.
24. Yu F, Yao H, Zhu P, *et al*. let-7 regulates self renewal and tumorigenicity of breast cancer cells. *Cell* 2007; **131**: 1109–1123.
25. Zhao Y, Deng C, Wang J, *et al*. *Let-7* family miRNAs regulate estrogen receptor alpha signaling in estrogen receptor positive breast cancer. *Breast Cancer Res Treat* 2011; **127**: 69–80.
26. Ellis MJ, Tao Y, Luo J, *et al*. Outcome prediction for estrogen receptor-positive breast cancer based on postneoadjuvant endocrine therapy tumor characteristics. *J Natl Cancer Inst* 2008; **100**: 1380–1388.
27. Li J, Smyth P, Flavin R, *et al*. Comparison of miRNA expression patterns using total RNA extracted from matched samples of formalin-fixed paraffin-embedded (FFPE) cells and snap frozen cells. *BMC Biotechnol* 2007; **7**: 36.
28. Si ML, Zhu S, Wu H, *et al*. miR-21-mediated tumor growth. *Oncogene* 2007; **26**: 2799–2803.
29. Zhao JJ, Lin J, Yang H, *et al*. MicroRNA-221/222 negatively regulates estrogen receptor alpha and is associated with tamoxifen resistance in breast cancer. *J Biol Chem* 2008; **283**: 31079–31086.
30. Garcia-Casado Z, Guerrero-Zotano A, Llombart-Cussac A, *et al*. A polymorphism at the 3′-UTR region of the aromatase gene defines a subgroup of postmenopausal breast cancer patients with poor response to neoadjuvant letrozole. *BMC Cancer* 2010; **10**: 36.

SUPPORTING INFORMATION ON THE INTERNET

The following supporting information may be found in the online version of this article:

Figure S1. Ki-67 proliferation index (%) of pre-AI and post-AI treatment in the patients.

Estrogen receptor α and β in esophageal squamous cell carcinoma

Masashi Zuguchi,[1,2] Yasuhiro Miki,[1] Yoshiaki Onodera,[1] Fumiyoshi Fujishima,[3] Daisuke Takeyama,[1,2] Hiroshi Okamoto,[2,3] Go Miyata,[2] Akira Sato,[2] Susumu Satomi[2] and Hironobu Sasano[1,3,4]

[1]Department of Pathology, [2]Division of Advanced Surgical Science and Technology, Tohoku University Graduate School of Medicine, Sendai, Miyagi, [3]Department of Pathology, Tohoku University Hospital, Sendai, Miyagi, Japan

(Received January 12, 2012/Revised March 21, 2012/Accepted March 22, 2012/Accepted manuscript online March 29, 2012)

A gender difference has been reported in the morbidity of esophageal squamous cell carcinoma (ESCC). Estrogens have been proposed to play a role in this difference but the details have not yet been clarified. Therefore, in the present study, we examined the status of estrogen receptor (ER)α and ERβ in 90 Japanese ESCC patients. ERα and ERβ immunoreactivity was detected in the nuclei of ESCC cells (41.1 and 97.8%, respectively). There was a significant positive association between the ERβ H score and histological differentiation ($P = 0.0403$), TNM-pM (LYM) ($P = 0.00164$) and Ki67/MIB1 LI of carcinoma cells ($P = 0.0497$, $r = 0.207$). In addition, the ERβ status of carcinoma cells was significantly correlated with unfavorable clinical outcome of the patients. Multivariate analysis further revealed the ERβ status in carcinoma cells as an independent unfavorable prognostic factor of these patients. We further examined the effects of estrogen treatment on ESCC cell line (ECGI-10) transfected with ERα or ERβ *in vitro*. The number of ECGI-10 transfected with ERβ was increased by estradiol or ERβ specific agonist but estradiol did not exert any effect upon the cell number of ECGI-10 transfected with ERα. In summary, the results of the present study clearly demonstrate that the status of ERβ in ESCC was closely associated with the unfavorable prognosis, possibly through altering cell proliferation of carcinoma cells. (*Cancer Sci*, doi: 10.1111/j.1349-7006.2012.02288.x, 2012)

Human esophageal squamous cell carcinoma (ESCC) is one of the most aggressive malignancies, despite recent marked improvement of therapeutic techniques and perioperative management. Results of most epidemiological studies demonstrate prominent gender differences in the prevalence of ESCC. ESCC is generally more common in men than women, with a male to female ratio of approximately 6:1 in Japan.[1] In addition, the prognosis of ESCC patients is reported to be significantly better in women than in men following an adjustment of various clinicopathological factors.[2] Several reported studies also suggest the possible roles of estrogens in development of ESCC.[3,4]

Sex steroids, such as estrogen, are well-known to contribute to physiological maturation and cell proliferation of estrogen dependent tissues, such as breast and endometrial tissues. Estrogens also play important roles in many non-gonadal or non-classical estrogen' receptors' dependent tissues in both men and women through estrogen receptors (ER). Therefore, it is important to examine the status of ER in these tissues. Two different isomers of ER, ERα and β, were first identified by Enmark *et al.*[5] Both ERα and ERβ are encoded by ESR1 located on chromosome 6q25[6] and ESR2 located on chromosome 14q22-24,[7] respectively. Estrogens have also been reported to play pivotal roles in several types of human malignancies, which had not been necessarily considered as classical estrogen-dependent neoplasms, such as those arising in lung,[8,9] urinary bladder[10] and gastrointestinal tract.[11,12] ERwere also reported to be detected in laryngeal and ESCC.[13–17] Nozoe *et al.* report that the group of the patients associated with cytoplasmic ERα-positive/nuclear ERβ-negative status was associated with a significant adverse clinical outcome in 73 cases of ESCC.[13] Kalayarasan *et al.* also report that the status of ERβ in carcinoma cells was correlated with poor histological differentiation and advanced clinical stages in ESCC patients.[15] These reported findings all suggest that estrogens are considered to be at least involved in biological behavior of ESCC through ER present in carcinoma cells. However, it is also true that controversy exists regarding the biological and clinical significance of estrogens in ESCC.[17]

Therefore, in the present study, we attempted to evaluate estrogen actions through ERα and ERβ in ESCC as follows. We first examined the status of ERα and ERβ using immunohistochemistry in 90 Japanese ESCC cases and evaluated their correlation with clinicopathological findings of individual patients, including overall survival or disease-free survival. We further characterized the potential biological functions of ERα and ERβ in ESCC cell lines stably transfected with ERα or ERβ.

Materials and Methods

Patients and tissue preparation. A total of 90 specimens of thoracic ESCC were obtained from Japanese patients who underwent potentially curative esophagectomy with lymph node dissection from 2000 to 2005 at the Second Department of Surgery at Tohoku University Hospital (Sendai, Japan). These patients had received neither chemotherapy nor irradiation therapy prior to surgery. These 77 men and 13 women had a median age of 63.9 years (range, 37–81 years). A total of 18 specimens of non-neoplastic epithelium were also obtained from these 90 cases. These specimens had been fixed with 10% formalin for 36–48 h at room temperature and embedded in paraffin wax. Relevant clinical data were retrieved from careful review of the patients' charts. Histopathological features of all the tumors were independently reviewed by four of the authors (M. Z., D. T., F. F. and H. S.). The pathological stage of each cancer was defined according to the TNM system and each lesion was graded histologically according to the World Health Organization classification. The median follow-up time was 65.5 months (range, 1–119 months). The research protocol in this study was approved by the Ethics Committee at the Tohoku University School of Medicine (Accesssion No. 2009-453) and informed consent was obtained from each patient before surgery.

Immunohistochemistry. Mouse monoclonal antibodies for ERα(6F11), ERβ(14C8) and Ki-67 (MIB1) were purchased

[4]To whom correspondence should be addressed.
E-mail: hsasano@patholo2.med.tohoku.ac.jp

doi: 10.1111/j.1349-7006.2012.02288.x

from Novocastra (Newcastle, UK), Gene Tex (San Antonio, TX, USA) and DAKO (Carpinteria,CA, USA), respectively.

Serial 4-μm thick tissue sections were deparaffinized with xylene and ethanol. Antigen retrieval was performed by heating the slides in an autoclave at 121°C for 5 min in citric acid buffer (2 mmol/L citric acid and 9 mmol/L trisodium citrate dehydrate, pH 6.0) or instant antigen retrieval H buffer (Mitsubishi Kagaku Iatron, Tokyo, Japan) for ER. Sections were then incubated with 10% normal rabbit serum for the monoclonal antibodies to reduce nonspecific background immunostaining. All incubations were performed for 18 h at 4°C with primary antibodies. The dilutions of primary antibodies were summarized as follows: ERα, 1:50; ERβ, 1:1000; and Ki-67, 1:100. Endogenous peroxidase activity was blocked by immersing the slides in 0.3% hydrogenperoxidase for 30 min at room temperature. The sections were subsequently incubated with biotinylated rabbit antimouse IgG (Histofine Kit; Nichirei, Tokyo, Japan). The localization of ER was then visualized with 3-Amino-9-ethylcarbazole and counterstained with hematoxylin. The other antigen-antibody complex was then visualized with 3.3-diaminobenzidine (1 mmol/L, in 50 mol/L Tris–HCl buffer, pH 7.6 and 0.006% H_2O_2) and counterstained with hematoxylin. ERα positive breast cancer tissue was used as a positive control for ERα. Non-pathologic prostate tissue was used as a positive control for ERβ. As a negative control, normal mouse or rabbit IgG was used instead of the primary antibodies and no specific immunoreactivity was detected in these preparations.

Evaluation of immunoreactivity. We evaluated the nuclear immureactivity of ERα, ERβ and Ki67. The immunoreactivities for ERα and Ki67 were evaluated in approximately 1000 carcinoma cells in each case and the percentage of immunoreactivity (i.e. labeling index [LI]) was determined after counting. In the present study, we used the H score for semiquantitative analysis of nuclear ERβ immunoreactivity.[18] Approximately 1000 tumor cells were counted in three different representative areas of carcinoma infiltration in each case and the H score was derived from the formula: H score = (percentage of strongly stained nuclei × 3) + (percentage of moderately stained nuclei × 2) + (percentage of weakly stained nuclei × 1). Scoring was performed independently by three of the authors (M. Z., D. T. and F. F.). When the inter-observer differences were <5%, the mean value was obtained as a final value of LI and H score. When the differences were more than 5%, all of the examiners evaluated the immunohistochemical findings simultaneously through multi-headed light microscopy and reached a consensus. When evaluating the possible correlation between ERβ status and clinical outcome of individual patients, the cases were tentatively classified into two groups according to their ERβ H scores (high ERβ, ≥250 H score; low ERβ, 0–249 H score, respectively), because ERβ H scores were found to be distributed in a peak on the boundary of approximately 250 (data not shown). In addition, the median value of the ERβ H score was 231.2, near the value of 250. The selection of the median value as the cut-off point was reported to secure objectivity because it is not determined as an "optimal" cut-off point.[19,20]

Cell culture and chemicals. Human ESCC cell line EC-GI-10 was provided by RIKEN Bioresource Center (Tsukuba, Japan). TE-1, TE-4 and TE-8 were obtained from the Cell Resource Center for Biomedical Research, Institute of Development, Aging and Cancer, Tohoku University (Sendai, Japan). All ESCC cell lines were cultured in RPMI 1640 (Sigma-Aldrich, St. Louis, MO, USA) with 10% FBS (Nichirei, Tokyo, Japan). In this study, cells were cultured with phenol red-free RPMI 1640 containing 10% dextran coated charcoal treated FBS for 3 days before the experiment. 17β-estradiol was purchased from Sigma-Aldrich. An ERα selective agonist (propyl-pyrazole-triol; PPT),[21] an ERβ selective agonist (diarylpropionitrile [DPN])[21] and a pure ER antagonist, ICI 182780,[22] were purchased from Tocris Bioscience (Minneapolis, MN, USA).

Stable transfection: establishment of EC-GI-10 cells expressing ERα or ERβ. The transformed ECGI-10 cells expressing ERα (EC-GI-10 + ERα) or ERβ (EC-GI-10 + ERβ) were established to further characterize the biological functions of ER isoforms in ESCC.

Stable transfection was performed according to the methods reported in previous studies with some modifications.[8,23,24] ERα and ERβ expression vectors for ERα (pRc/CMV-ERα) and ERβ (pRc/CMV-ERβ) used in this study were described previously.[8,23,24] Briefly, EC-GI-10 cells were transfected with ERα or ERβ expression vector with Lipofectamine LTX (Invitrogen Life Technologies, Gaithersburg, MD, USA). After 24 h in culture, the cells were subsequently grown in fresh RPMI 1640 supplemented with 10% FBS containing 1 mg/mL geneticin (G418; Sigma-Aldrich) for 2 weeks. Isolated colonies were trypsinized in metal ring cups and the cells were further cultured in the presence of 200 μg/mL G418. As a negative control, empty vector was also transfected in the EC-GI-10 cells. Expression of ERα and ERβ at both mRNA and protein levels in EC-GI-10 cells was examined by quantitative RT-PCR and immunohistochemistry.

RT-PCR. Total RNA was carefully extracted from human ESCC cell line (EC-GI-10, TE-1, TE-4 and TE-8) using the TRIzol (Invitrogen Life Technologies) method. The QuantiTect Reverse Transcription kit (Qiagen, Hilden, Germany) was used in the synthesis of cDNA. RT-PCR was carried using the Light-Cycler System (Roche Diagnostics, Manheim, Germany), and ribosomal protein L 13a (RPL13A) was also used as an internal standard. The primer sequences used in this study are as follows: ERα(NM_000125); forward: 5′-AGACACTTTGATCCACCTGA-3′ (cDNA position 1811–1831) and reverse: 5′-CAAGGAATGCGATGAAGTAG-3′ (cDNA position 2080–2100), ERβ (AB006590); forward: 5′-CCTGGCTAACCTCCTGATGC-3′ (cDNA position 1460–1480) and reverse: 5′-ACCCCGTGATGGAGGACTT-3′ (cDNA position 1608–1627) and RPL13A (NM_012423); forward: 5′-CCTGGAGAGAAG AGGAAAGAGA-3′ (cDNA position 487–509) and reverse: 5′-TTGAGGACCTCTGTGTATTTGTCAA-3′ (cDNA position 588–612). The PCR products were purified and subjected to direct sequencing to verify amplification of the correct sequences. Negative controls, in which the reaction mixture lacked cDNA template, were included to exclude the possibility of exogenous contaminant DNA.

cDNA of known concentrations for target genes and the housekeeping gene RPL13A were used to generate standard curves for real-time quantitative PCR to determine the quantity of target cDNA transcript. The Ct (cycle threshold) values were used to calculate the gene-specific input mRNA amounts according to the calibration curve method. The mRNA level in each case was represented as a ratio of RLP13A and was evaluated as a ratio (%) compared with that of each control.[8,20,25]

Cell proliferation assays. EC-GI-10 including its transformants and TE-1, TE-4 and TE-8 were treated with the indicated compounds for 3 days and the cell proliferation was measured by a WST-8 [2-(2-methoxy-4-nitrophenyl)-3-(4-nitrophenyl)-5-(2,4-disulfophenyl)-2H-tetrazolium, monosodium salt] method using Cell Counting Kit-8 (Dojin Kagaku, Kumamoto, Japan).[8,26]

Statistical analysis. The values for ERβ H score, patient age, tumor size, Ki67/MIB1 LI and ERα LI were demonstrated as mean ± SEM. The statistical analyses between ERβ H score and clinicopathological parameters of individual patients were evaluated using the Mann–Whitney *U*-test, the Kruskal–Wallis test, a correlation coefficient (*r*) and regression equations when appropriate.

Overall survival (OS) and disease-free survival (DFS) curves of the patients examined were generated according to the

doi: 10.1111/j.1349-7006.2012.02288.x

Kaplan–Meier method and statistical significance was calculated using the log-rank test. Cox's proportional hazard model was used for both univariate and multivariate analyses.

The proliferation activity was evaluated as a ratio (%) compared to that of controls (no treatment with either estradiol for 72 h). The statistical analyses between relative luciferfase activity and each agent were evaluated using the Kruskal–Wallis test and the Scheffe test.

Statistical differences were examined using StatView 5.0 J software (SAS Institute, Cary, NC, USA) and values of $P < 0.05$ were considered statistically significant.

Results

Immunohistochemistry: ERα and ERβ status in non-neoplastic esophagus and esophageal squamous cell carcinoma. Both ERα and ERβ immunoreactivity were detected in the nuclei of non-neoplastic basal layer cells of the esophagus (Fig. 1a,b). ERα immunoreactivity was detected in the nuclei of carcinoma cells in 38/90 ESCC (Fig. 1c). The mean value of the ERα labeling index in 90 ESCC was 22.3 ± 3.2 (range, 0–90). ERβ immunoreactivity was detected in the nuclei of carcinoma cells with a variety of immunointensity in 88/90 ESCC (Fig. 1d). The mean value of the ERβ H score in 90 ESCC was 208.9 ± 7.4 (range, 0–295).

Correlation between the status of ERα immunoreactivity and clinicopathological variables in 90 esophageal squamous cell carcinoma patients. Associations between ERα status and clinicopathological variables of the patients examined are summarized in Table 1. No significant association was detected between ERα status and age, gender, tumor size, depth of tumor invasion, presence of lymph node metastasis, TNM stage, lymphatic invasion, venous invasion, infiltrative growth pattern and the Ki67/MIB1 Labeling index status of the patients examined.

Correlation between the status of ERβ immunoreactivity and clinicopathological variables in 90 esophageal squamous cell carcinoma patients. Associations between ERβ status and clinicopathological variables of the individual patients examined are summarized in Table 1. There was a statistically significant positive association between ERβ H score and tumor differentiation ($P = 0.0403$) and TNM-pM (LYM) ($P = 0.0164$). There was also a weak but statistically significant positive correlation between the ERβ H score and Ki67/MIB1 LI ($P = 0.0497$, $r = 0.207$). No significant association was detected between ERβ immunoreactivity and age, gender, tumor size, depth of tumor invasion, presence of lymph node metastasis, TNM stage, lymphatic invasion, venous invasion or infiltrative growth pattern of the patients examined in the present study.

Correlation between ERα status and clinical outcome in 90 esophageal squamous cell carcinoma patients. The OS and DFS curves of the patients examined are summarized in Figure 2(a, b), respectively. The patients with positive nuclear ERα immunoreactivity in carcinoma cells were by no means associated with better survival or favorable clinical outcome (log-rank test: OS, $P = 0.4660$; DFS, $P = 0.3468$).

Correlation between ERβ status and clinical outcome in 90 esophageal squamous cell carcinoma patients. The OS and DFS curves of the patients examined are illustrated in Figure 2(c, d), respectively. In the present study, the patients with high nuclear ERβ immunoreactivity were significantly associated with shorter survival or adverse clinical outcome (log-rank test: OS, $P = 0.0017$; DFS, $P = 0.0005$). Results of univariate analysis (Table 2) demonstrated that pathological stage (OS, $P = 0.0003$; DFS, $P = 0.0006$), ERβ status in the nucleus of carcinoma cells (OS, $P = 0.0025$; DFS, $P = 0.0010$), tumor size (OS, $P = 0.0485$; DFS, $P = 0.0366$) and infiltration type (OS, $P = 0.0200$; DFS, $P = 0.0416$) were all significant prognostic factors for OS and/or DFS in 90 ESCC examined in our study. A subsequent multivariate analysis did reveal that ERβ status (OS, $P = 0.0010$; DFS, $P = 0.0007$) was an independent prognostic factor for OS and DFS of these patients, as well as pathological stage (OS, $P = 0.0019$; DFS, $P = 0.0091$) and infiltration type (OS, $P = 0.0185$; DFS, $P = 0.0328$).

Establishment of EC-GI-10 esophageal squamous cell carcinoma cells expressing ERα or ERβ. The transformed EC-GI-10 ESCC cells expressing ERα (EC-GI-10 + ERα) or ERβ (EC-GI-10 + ERβ) were established because the parental EC-GI-10 cells and TE-1, TE-4 and TE-8 cells examined in this study expressed only miniscule amounts of ERα or ERβ at mRNA levels (data not shown). Estradiol administration (1 pmol/L–100 nmol/L) did not change the number of cells even after 72 h in all the cell lines, TE-1, TE-4, TE-8 and EC-GI-10 (data not shown). As a control, we also isolated a clone

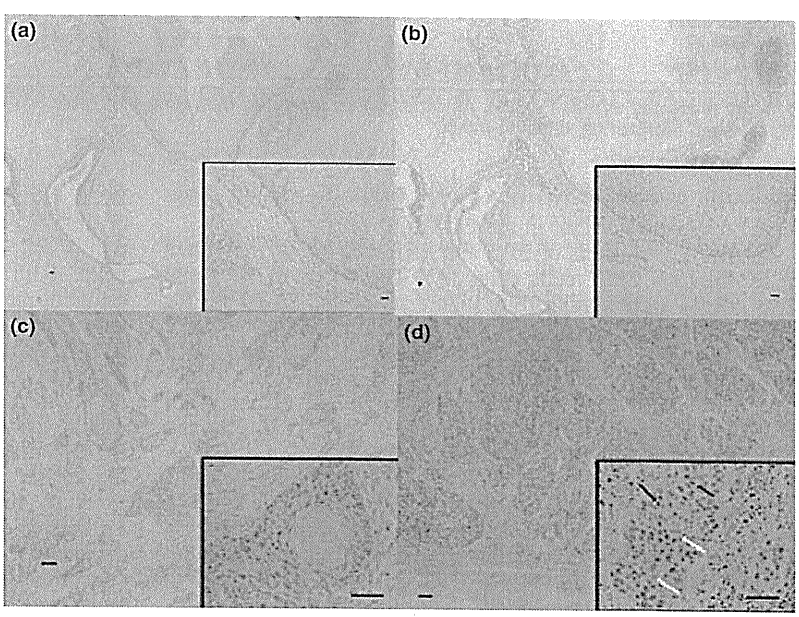

Fig. 1. Representative illustrations of immunohistochemistry in human esophageal squamous cell carcinoma. (a) Estorogen receptor α (ERα) immunoreactivity was detected in the nuclei of non-neoplastic epithelial cells. (b) Estorogen receptor β (ERβ) immunoreactivity in the nuclei of non-neoplastic epithelial cells. (c) ERα immunoreactivity in esophageal squamous cell carcinoma (ESCC) case. (d) ERβ immunoreactivity in ESCC case. Black arrows represent marked immunoreactivity (+++) of ERβ and white arrows represent weak immunoreactivity (+) of ERβ. Bar represents 100 μm.

Table 1. Correlation between ERα and ERβ and clinicopathological variables in 90 esophageal squamous cell carcinoma patients

Variable	*n* or mean ± SEM	Nuclear ERα		Nuclear ERβ	
		Labeling		Index H score	
		Mean ± SEM	*P*-values	Mean ± SEM	*P*-values
Age (years)					
<65	48	22.2 ± 4.5	0.5991	201.0 ± 10.3	0.1929
≥65	42	22.4 ± 4.7		218.3 ± 10.5	
Gender					
Male	77	22.6 ± 3.5	0.6298	209.2 ± 7.9	0.7786
Female	13	20.5 ± 9.0		206.8 ± 21.8	
Tumor size (mm)					
<50	54	25.9 ± 4.5	0.2439	208.3 ± 10.2	0.6329
≥50	36	17.0 ± 4.4		209.7 ± 10.6	
TNM-pT					
pT1	29	28.7 ± 6.5	0.4309	202.2 ± 16.5	0.2148
pT2	11	25.8 ± 9.3		206.7 ± 15.4	
pT3	47	19.0 ± 4.1		209.8 ± 9.1	
pT4	3	0.0		266.2 ± 13.3	
TNM-pN					
pN0	36	27.0 ± 5.5	0.3130	200.3 ± 13.1	0.6565
pN1	54	19.2 ± 3.9		214.6 ± 8.7	
TNM-pM					
pM0	81	23.8 ± 3.5	0.3569	203.7 ± 7.9	0.0164**
pM1 (LYM)	9	8.5 ± 6.8		255.4 ± 10.4	
TNM-pStage					
I	19	36.2 ± 8.4	0.2381	198.2 ± 20.8	0.0580
II	31	7.6 ± 5.1		195.5 ± 12.5	
III	31	22.5 ± 5.3		215.3 ± 10.8	
IV	9	8.5 ± 6.8		255.4 ± 10.4	
Differentiation					
Well	17	11.5 ± 4.9	0.0688	188.2 ± 23.4	0.0403**
Mod	59	20.5 ± 4.0		205.2 ± 8.5	
Poorly	14	43.0 ± 9.1		249.4 ± 7.8	
Lymphatic invasion					
Negative	35	24.2 ± 5.8	0.8167	218.3 ± 11.3	0.1288
Positive	55	21.1 ± 3.8		202.9 ± 9.7	
Venous invasion					
Negative	31	26.2 ± 5.5	0.4223	209.7 ± 13.6	0.5810
Positive	59	20.3 ± 4.0		208.4 ± 8.8	
Growth pattern					
Expansive	26	21.3 ± 6.1	0.4961	224.4 ± 12.6	0.1039
Intermediate	52	20.4 ± 4.2		198 ± 10.0	
Infiltrative	12	32.9 ± 8.9		222.4 ± 20.4	
Ki-67 LI (%)	43.7 ± 2.0 (8.1–83.9)	0.8412 (r = 0.021)		0.0497** (r = 0.207)	

Data are presented as mean ± SEM. All other values represent the number of cases. **P-values less than 0.05 were considered significant.
ER, estrogen receptor; LI, labeling index.

tentatively termed EC-GI-10 + CMV, which was stably transfected with empty vector in the EC-GI-10 cells.

Relatively low levels of ERα and ERβ mRNA were detected in EC-GI-10 + CMV cells (Fig. 3A). The levels of ERα and ERβ mRNA were significantly higher in the EC-GI-10 + ERα and + ERβ cells, respectively, than those in EC-GI-10 + CMV cells (Fig. 3A). In immunohistochemistry, ERα and ERβ immunoreactivity was relatively weak or negative in EC-GI-10 + CMV cells (Fig. 3B). Immunoreactivity of ERα but not of ERβ was detected in EC-GI-10 + ERα cells (Fig. 3B) and vice versa in EC-GI-10 + ERβ cells (Fig. 3B).

Effects of ERα or ERβ expression on estradiol, propyl-pyrazole-triol and diarylpropionitrile-mediated cell proliferation in EC-GI-10 cells. The number of EC-GI-10 + ERα cells was significantly decreased following the treatment with PPT (1 μmol/L), but not with estradiol (1 μmol/L) or DPN (1 μmol/L) compared to that administered with vehicle control cells (Fig. 3C, left). Both estradiol (1 μmol/L) and ERβ specific agonist DPN (1 μmol/L) treatments significantly increased the cell proliferation of EC-GI-10 + ERβ cells when compared to that administered with vehicle control cells (Fig. 3C, center). The estradiol-mediated cell proliferation of EC-GI-10 + ERβ cells was significantly suppressed ($P < 0.001$) by the addition of ICI 182780 (100 pmol/L) and reached the control level. There was no significantly difference in the number of EC-GI-10 + CMV cells treated with estradiol, DPN or TTP (Fig. 3C, right). Estradiol-mediated cell proliferation was detected in EC-GI-10 + ERβ cells and was significantly induced following the treatment with 1 nmol/L to 1 μmol/L estradiol (the difference of groups; Kruskal–Wallis, $P = 0.0004$, NC v 1 nM to 1 μM have difference in Scheffe test; Fig. 3D, right). Estradiol decreased the cell proliferation of EC-GI-10 + ERα in the concentration of 1 pmol/L to 1 μmol/L, but this increment did not reach statistical significance (Fig. 3D, left)

doi: 10.1111/j.1349-7006.2012.02288.x